Review

Helen Julian, Novesa Nurgirisia, Putu Doddy Sutrisna and I. Gede Wenten*

Advances in seawater membrane distillation (SWMD) towards stand-alone zero liquid discharge (ZLD) desalination

https://doi.org/10.1515/revce-2020-0073
Received September 16, 2020; accepted March 12, 2021;
published online May 18, 2021

Abstract: Seawater membrane distillation (SWMD) is a promising separation technology due to its ability to operate as a stand-alone desalination unit operation. This paper reviews approaches to improve laboratory-to-pilot-scale MD performance, which comprise operational strategies, module design, and specifically tailored membranes. A detailed comparison of SWMD and sea water reverse osmosis is presented to further analyze the critical shortcomings of SWMD. The unique features of SWMD, namely the ability to operate with extremely high salt rejection and at extreme feed concentration, highlight the SWMD potential to be operated under zero liquid discharge (ZLD) conditions, which results in the production of high-purity water and simultaneous salt recovery, as well as the elimination of the brine disposal cost. However, technical challenges, such as thermal energy requirements, inefficient heat transfer and integration, low water recovery factors, and lack of studies on real-case valuable-salt recovery, are impeding the commercialization of ZLD SWMD. This review highlights the possibility of applying selected strategies to push forward ZLD SWMD commercialization. Suggestions are projected to include intermittent removal of valuable salts, in-depth study on the robustness of novel membranes, module and configuration, utilization of a low-cost heat exchanger, and capital cost reduction in a renewable-energy-integrated SWMD plant.

Keywords: desalination; energy consumption; membrane distillation; water cost; zero liquid discharge.

1 Introduction

Water scarcity presents serious global challenges from an increase in population, industrialization, and climate change, with more than 33% of the world population currently living in water-stressed places (González et al. 2017). In addition, the production of clean water has caused the overexploitation of groundwater and nearby river systems. Hence, to enable a sustainable life cycle, the needs to employ saltwater to produce a supply of fresh water has motivated many industries in many countries to deploy desalination processes to produce directly fresh or potable water from seawater.

Well-established desalination technologies, such as multi effect distillation (MED), multistage flash distillation (MSF), and reverse osmosis (RO), have led the desalination market. MED and MSF are classified as thermal desalination methods, utilizing steam to heat seawater to its boiling temperature and evaporate the water. While high-quality water can be produced, the discharge temperature of MSF and MED is higher than the environment, disrupting marine life and the ecosystem. Besides, scaling and high energy are required, motivating the development of other desalination technologies. Nowadays, 80% of desalination plants worldwide use RO technology. Continuous research to increase efficiency with regard to cost and energy has resulted in RO becoming the most energy-efficient technology at present.

While RO water recovery has increased, high osmotic pressure remains the main obstacle in its application. Moreover, in addition to fresh water, seawater reverse osmosis (SWRO) produces a huge amount of brine, disposal of which presents another serious challenge. Recently,

***Corresponding author: I. Gede Wenten,** Chemical Engineering Department, Institut Teknologi Bandung (ITB), Jalan Ganesha 10, Bandung 40132, Indonesia; and Research Center for Nanosciences and Nanotechnology, Institut Teknologi Bandung, Jalan Ganesha 10, Bandung 40132, Indonesia, E-mail: igw@che.itb.ac.id. https://orcid.org/0000-0002-5818-9286
Helen Julian and Novesa Nurgirisia, Chemical Engineering Department, Institut Teknologi Bandung (ITB), Jalan Ganesha 10, Bandung 40132, Indonesia, E-mail: helen@che.itb.ac.id (H. Julian), novesa.nurgirisia@gmail.com (N. Nurgirisia)
Putu Doddy Sutrisna, Department of Chemical Engineering, Universitas Surabaya, Kalirungkut-Surabaya, Indonesia, E-mail: pudod@staff.ubaya.ac.id

membrane distillation (MD) has gained significant attention as a potential alternative to the desalination process, as the presence of high osmotic pressure is eliminated in MD (Hettiarachchi 2015). In addition, the potential of MD for mineral recovery in the concentrate has been considered as another beneficial effect of MD to create a zero liquid discharge (ZLD) system. Membrane distillation is a thermally driven separation process employing a hydrophobic microfiltration membrane as a barrier between the feed and permeate stream (Hettiarachchi 2015; Salmon and Luis 2018). The driving force of the separation process is the vapor pressure difference between the feed and permeate streams (Lawson and Lloyd 1997). Due to membrane hydrophobicity, the water in the feed solution travels in the form of vapor through the pores of the membrane (Jabed et al. 2016). The feed solution does not necessarily need to be heated to the boiling point to generate water vapor, as the process can be carried out at feed temperatures as low as 30 °C, which is significantly lower than other thermal desalination technologies (Alkhudhiri et al. 2012; Lawson and Lloyd 1997; Pantoja et al. 2016). In addition, unlike other membrane desalination processes, 100% theoretical solute rejection can be achieved in the MD operation (Cath et al. 2004; Lagana et al. 2000; Patil and Shirsat 2017). As MD operation is based on a vapor pressure gradient, the operation is not limited by osmotic pressure, allowing operation at high feed concentration, where RO fails to maintain its performance. While MD is a relatively new technology for the application of seawater desalination, seawater membrane distillation (SWMD) has gained much attention, as indicated by the increasing number of publications (Figure 1).

Studies on the applicability of SWMD for ZLD desalination are limited and most studies utilize brine water of other water sources with a high salt concentration as the feed. The results indicated the possibility of increasing the freshwater recovery factor to up to 95% and recovering 78% of NaCl from nanofiltration (NF) retentate. In the bench-scale membrane distillation–crystallization (MDC) experiment carried out with RO brine as the feed, NaCl crystal production of 17 kg/m^3 was achieved with 90% water recovery (Ji et al. 2010). Using synthetic SWRO brine as the feed solution, Julian et al. studied the performance of submerged vacuum membrane distillation crystallization for salt recovery. The salt recovery ratio increased with the increase of initial feed concentration. At the initial feed TDS of 22 and 33 g/L, 40 and 45% of salt recovery were achieved, respectively (Julian et al. 2016). In another study, the application of fractional-submerged MDC (F-SMDC), which combines MD and crystallization in a single feed reactor with a submerged membrane, was investigated. The temperature gradient in the reactor was generated by setting a high temperature at the top of the reactor and a low temperature at the bottom of the reactor to induce crystal precipitation. Using a 120 g/L Na_2SO_4 feed solution, higher water and crystal recovery and lower membrane scaling were achieved compared to the conventional submerged-MD configuration. With the removal of 2495 mL of fresh water from the feed solution, 551 g of Na_2SO_4 crystal can be produced (Choi et al. 2018). In an MD pilot-scale setup, Ali et al. (2015) conducted experiments for salt and freshwater recovery from produced water. It was found that approximately 16.4 kg of NaCl can be obtained when treating 1 m^3 of produced water with 37% recovery.

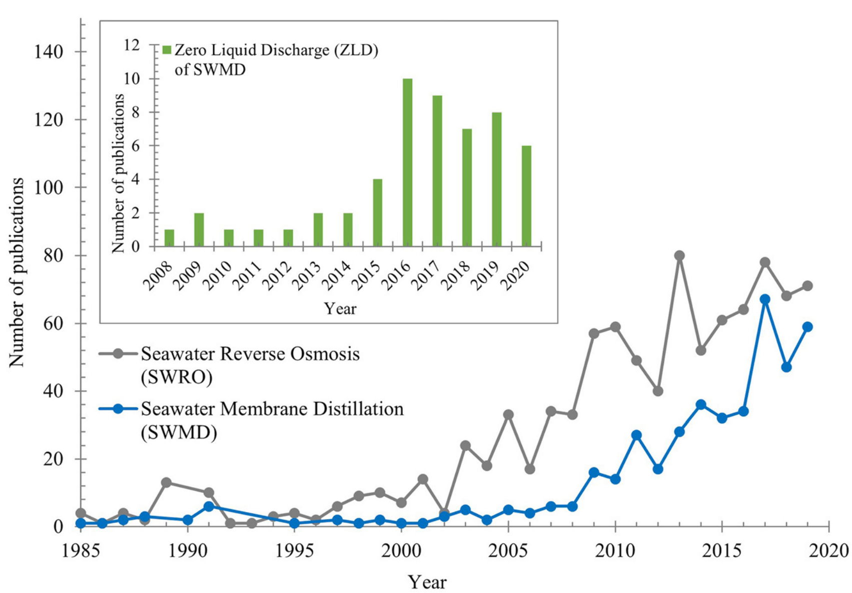

Figure 1: Comparison of the number of publications related to SWRO and SWMD, especially the increase in ZLD SWMD research for seawater desalination, indexed by Scopus.

In another study, MD was integrated with other membrane technology such as RO and NF to produce water and minerals from seawater. This system was capable of producing 174,000,000 m^3 of potable water, extracting one ton of nickel from seawater (Quist-Jensen et al. 2016). Integration of MD with freeze desalination has also gained interest. In a recent study, freeze desalination and vacuum membrane distillation (FD-VMD) were combined for seawater desalination. The first stage of water recovery was conducted by FD, in which the clean ice was harvested, with liquified natural gas (LNG) regasification process as the energy provider. The concentrated brine from FD was then treated in vacuum membrane distillation (VMD) to increase the water recovery (Chung et al. 2014). Further integration of FD–MD with crystallizer was investigated to attain ZLD operation. The brine from MD was processed in a crystallizer to produce water and salt crystals at a rate of 69.48 and 2.52 kg/day, respectively. Energy for heating the feed solution can be obtained from the solar panel, while the energy for cooling to be used in FD and crystallizer was supplied from the regasification of LNG (Lu et al. 2019b).

While many studies showed promising salt and water recovery, limitations exist and prohibit the industrial application of SWMD. In this paper, fundamental limitations obstructing the performance of the SWMD operation are briefly discussed. Accordingly, recent advancements in MD performance improvement, specifically in operational strategy, module configuration, and novel membrane material, are comprehensively reviewed. The opportunity to use SWMD as a stand-alone desalination unit, particularly when compared to SWRO, is then elaborated on. In particular, detailed discussions on fouling propensity, pretreatment complexity, energy requirements, and total water cost of MD operation are presented. Furthermore, the unique capabilities of SWMD in producing high-purity water and harvesting valuable salts in ZLD conditions, as well as the direct impact on the water production costs, are highlighted. Lastly, this paper provides an outlook for future ZLD SWMD implementation and suggests strategies for further improving SWMD operations.

2 Current challenges in SWMD

Operational challenges such as concentration polarization, temperature polarization, fouling, and wetting affect the SWMD productivity and compromise the permeate quality. In addition to the operational challenges, the energy requirement in SWMD has become a concern that deters the industrialization of SWMD.

2.1 Temperature polarization and concentration polarization

Temperature polarization and concentration polarization occur simultaneously in line with the heat transfer and mass transfer mechanisms in MD (Figure 2). Temperature polarization is the temperature difference between the bulk feed solution and the feed-membrane interface as well as between the bulk permeate solution and the permeate-membrane interface. Temperature polarization may occur due to water vapor transport through membrane pores and the lack of fluid shear rate on the boundary layer area. In MD operation, temperature polarization is not favorable, as it reduces the overall driving force for water vapor transport across the membrane. Temperature polarization can result in an 80% driving force reduction in the MD process (Chen et al. 2017). Consequently, selecting MD configuration capable of reducing the temperature polarization and heat

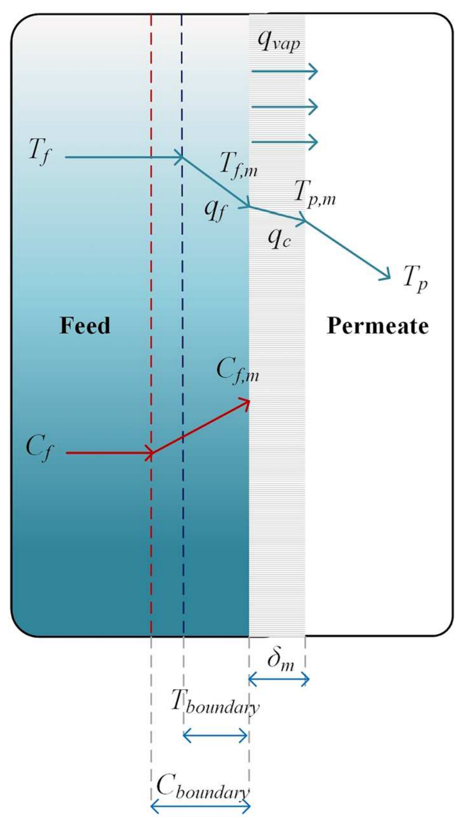

Figure 2: Schematic representation of mass and heat transfer in MD operation.

loss is crucial to increase the MD process's efficiency. Among the four basic MD configurations, VMD configuration can eliminate temperature polarization on the permeate side and reduce heat loss through conduction due to its very low pressure on the permeate side (Khayet et al. 2005).

Based on the study carried out by Guan et al. on equivalent energy cost, the VMD configuration could generate a 2.5-fold flux compared to the direct contact membrane distillation (DCMD) configuration (Tijing et al. 2016). In another study, a comparison of DCMD, air gap membrane distillation (AGMD), and VMD configurations using ceramic membranes suggested that the VMD configuration provided the highest permeate flux. This is attributed to the direct extraction of water vapor on the permeate side, which reduces heat loss by conduction and eliminates heat transfer in the permeate side boundary layer (Chen et al. 2018). Consequently, VMD is considered to be more efficient than DCMD or AGMD. Another test comparing DCMD and VMD configurations using polypropylene membranes and pure water as the feed showed that the VMD configuration has a significantly lower energy-consumption-to-permeate-flow-rate ratio, which underscores the superiority of VMD in term of energy efficiency (Ragunath et al. 2018). In general, the severity of temperature polarization is quantified as the temperature polarization coefficient (TPC), which depicts the ratio of the actual driving force to the theoretical value. A TPC of 1 indicates excellent and efficient heat transfer in the MD operation. However, practically, the TPC for MD ranges between 0.2 and 0.99, depending on the membrane module configuration (Burgoyne and Vahdati 2005; Cath et al. 2004; Gryta 2008b; Mericq et al. 2011; Schofield et al. 1987), and the TPC reductions become more significant with the increase in feed temperature (Burgoyne and Vahdati 2005; El–Bourawi et al. 2006; Mericq et al. 2011).

As the water vapor passes through the membrane, salts are accumulated in the feed-membrane boundary layer at a higher concentration than that of the bulk feed solution. This condition is referred to as concentration polarization (Jiang et al. 2017; Julian 2018; Lu et al. 2019b). While many studies suggest a minor effect of concentration polarization in the MD processes, particularly when compared to the temperature polarization, concentration polarization in the SWMD application remains unfavorable. Similar to temperature polarization, concentration polarization results in the reduction of vapor pressure for mass transport due to reduced water activity in the feed. The consequence of temperature polarization and concentration polarization is reduced water flux in the SWMD operation. Also, concentration polarization leads to supersaturation and initiates fouling of membrane surface (Drioli et al. 2004) at high solute concentrations.

2.2 Fouling

Membrane fouling, which is an accumulation of unwanted materials on the surface or inside the pores of a membrane, results in a decline in the overall performance of MD. If not addressed appropriately, this can lead to membrane damage, early membrane replacement, or even shutdown of the operation (Tijing et al. 2015). Similar to other membrane separation processes, the formation of fouling on the MD membrane needs to be controlled. Due to differences in membrane structure, design, and operating conditions, the mechanism of fouling in MD may be different from that of pressure-driven membrane processes. In seawater desalination, the foulants can be divided into three broad groups according to the fouling material (Meng et al. 2009): (a) inorganic fouling (scaling), (b) organic fouling, and (c) biological fouling (biofouling) (Figure 3). A nonporous fouling layer is likely to contribute to both thermal and hydraulic resistance, while a porous fouling layer may only increase thermal resistance (Alklaibi and Lior 2005).

Scaling occurs when there is deposition of salt crystals on the membrane surface. It is the most studied fouling in the SWMD application due to its severity, as seawater contains a high concentration of ions. Extensive research on SWMD scale formation indicated that sparingly soluble and negative temperature-solubility coefficient salts such as $CaSO_4$ and $CaCO_3$ are the deposited scale's major constituents, despite their low concentration in seawater (Curcio et al. 2010; He et al. 2009). The deposition of the salt crystals on the membrane surface occurs in two different mechanisms (Figure 4). In the first mechanism, both cations and anions are adsorbed on the membrane surface, which acts as the nucleation site for heterogeneous nucleation. As the cations and anions react, the nuclei are formed, followed by crystal growth. In the second mechanism, cations and anions react by means of homogeneous nucleation in the feed solution. The formed crystals precipitate out on the membrane surface, which is subsequently followed by crystal growth. Once the salt crystals are deposited on the membrane surface, they act as new nucleation sites, promoting the heterogeneous nucleation of other salts (such as MgSO4, NaCl, etc.) and exacerbate scaling. In addition, part of the growth crystals can detach from the membrane surface and transform into new nucleation sites for scaling in other areas of the membrane, resulting in rapid scale formation. In the

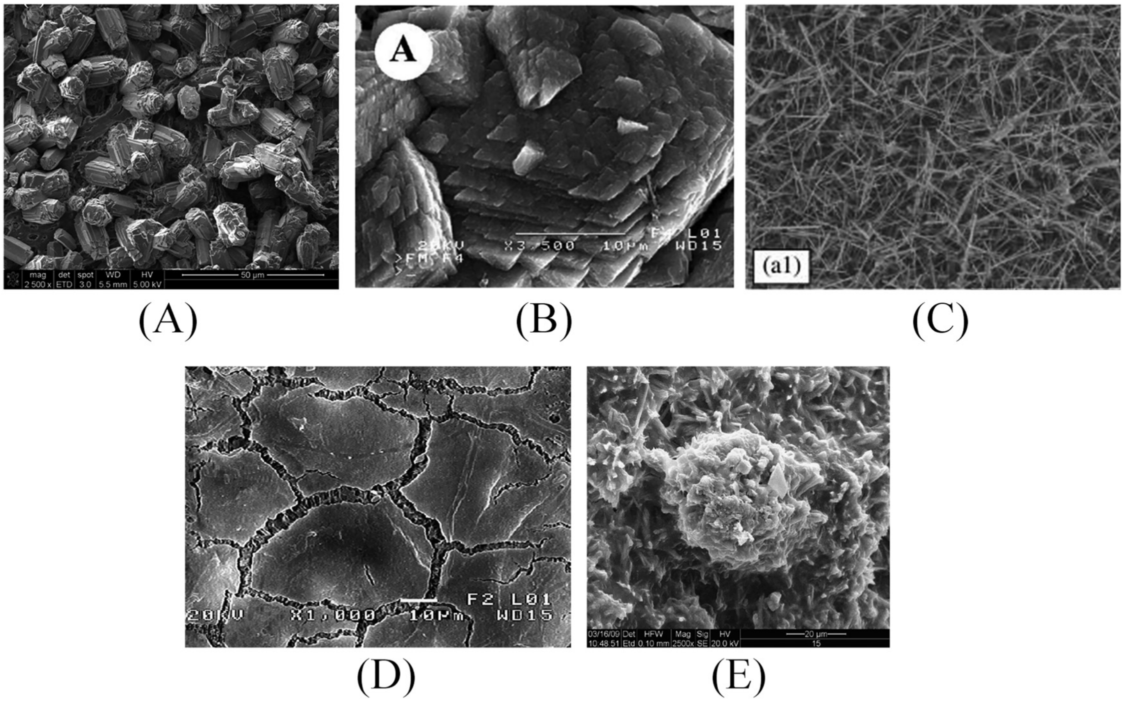

Figure 3: Fouling in SWMD such inorganic fouling: (A) calcium carbonate (Julian et al. 2016), reproduced with permission from Elsevier; (B) alkaline (Gryta 2008a), reproduced with permission from Elsevier; (C) gypsum (Nghiem and Cath 2011), reproduced with permission from Elsevier; (D) organic fouling: protein (Gryta 2008b), reproduced with permission from Elsevier; and (E) biofouling on polypropylene hollow fiber membrane (Tijing et al. 2015), reproduced with permission from Elsevier.

SWMD application, the flow velocity significantly affects the growth rate of the fouling layer as well as the morphology and size of the deposits. A higher flow velocity leads to the formation of smaller crystals and a porous deposit layer, while lower flow velocity produces thicker deposits in the form of "mountain-like" structures (Antony et al. 2011; Gryta 2009; Tijing et al. 2015).

Biofouling, or biofilm formation, occurs due to the growth of microorganisms on the membrane surface. Even though the biofouling process is slow and highly dependent on the environmental condition (e.g., nutrient content, temperature, ionic concentration, and light), the control of biofouling is challenging. Biofouling is possible with the presence of a single microorganism, as it can grow vegetatively to form a colony, which suggests the need for robust and effective pretreatment. In addition, during biofouling formation, the microorganisms secret extracellular polymeric substance (EPS) that acts as a barrier from chemical biocides and promotes nutrient storage (Maddah and Chogle 2017). Organic fouling mostly occurs due to the deposition of natural organic matter (NOM), which is mainly composed of humic acid (HA) (Deng et al. 2019). The deposited NOM can be adsorbed into the membrane pores, causing partial or full blockage and creating a gel-like structure on the membrane surface or binding with other particles to form a low-permeability particle-NOM layer on the membrane surface. In several studies, it was found that HA formed a fouling layer on the membrane surface; however, in other tests, HA penetration into the permeate side occurred, even without observed pore wetting due to the adsorption-desorption mechanism of HA through the membrane (Adusei–Gyamfi et al. 2019).

In practice, the occurrence of just one fouling mechanism is extremely rare as the seawater contains different components such as ions, microorganisms, and particulate and colloidal matter. The combined fouling mechanisms often exhibit a synergistic effect and any strategies to prohibit one particular fouling may exacerbate others. For example, pH adjustment of the feed to 4 is one of the strategies to inhibit $CaCO_3$ scale formation; however, low pH conditions promote the adsorption of HA macromolecules on the hydrophobic membranes. This then requires highly intensive treatment once the fouling layer forms on the membrane surface.

2.3 Wetting

In addition to fouling, membrane wetting is another challenge. Especially for long-term operations, progressive

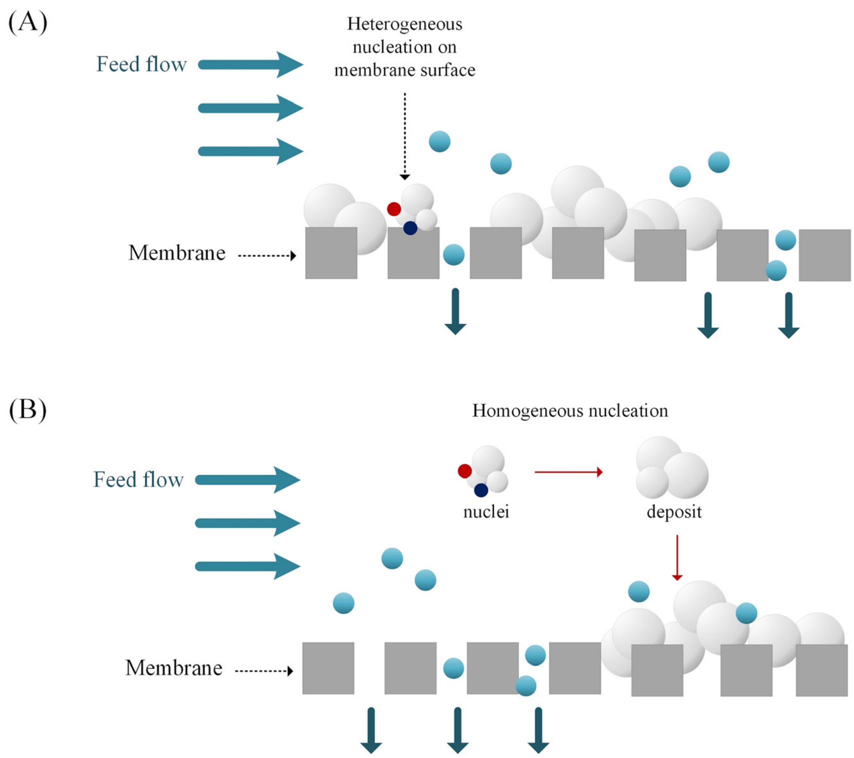

Figure 4: Scaling mechanism in SWMD by (A) heterogeneous and (B) homogeneous nucleation.

membrane wetting has been observed (Gryta 2005). Theoretically, MD has 100% salt rejection and only water vapor passes through the pores of the membranes; however, several factors such as poor long-term hydrophobicity of the material, membrane damage and degradation, extremely thin membranes, and the presence of foulants in the feed water can lead to pore wetting. The primary metric for measuring membrane wettability is liquid entry pressure (LEP). Membrane wetting can be placed into four categories: nonwetted, surface-wetted, partially-wetted, and fully-wetted. Surface wetting shifts the liquid/vapor interface inward on the membrane cross-section. Permeate flux may then decline gradually as a result of the associated increase in temperature polarization, which lowers the temperature of the evaporating interface in the pore (Gryta 2008b). In addition, scaling as a result of solvent evaporation can take place inside the pores in the vicinity of the meniscus (Gryta 2005). Partial wetting under certain conditions reduces the permeate flux due to a reduction in the active surface area for mass transport (Rezaei et al. 2018), or it can cause an increase in the permeate flux due to the wetting of some pores (i.e., vapor transport is overtaken by liquid transport), followed by a rapid decrease due to a steady blockage of pores by the foulants, depending on the experimental setup (Jansen et al. 2013). In the case of full wetting, the MD process no longer acts as a barrier, resulting in a viscous flow of liquid water through the membrane pores, incapacitating the MD process (Rezaei et al. 2018).

2.4 Energy consumption

The energy requirements limit the current application of SWMD, and many studies emphasize the need for waste heat as an energy source for MD application. In SWMD operation, both electrical energy and thermal energy are required. The electrical energy is used for fluid circulation and its requirement in SWMD can be evaluated by quantifying the specific electrical-energy consumption (SEEC), similar to the SWRO plant. The thermal energy is principally applied in SWMD for feed heating which creates the driving force for water vapor transport. The thermal energy requirement in SWMD can be quantified by the specific thermal-energy consumption (STEC), which indicates the amount of thermal energy required per unit volume of distillate water (kWh/m^3) (Zaragoza et al. 2014). Factor such as parasitic heat loss via conduction through the membrane materials increases the thermal energy requirement in SWMD. However, in a system with heat integration, recovery of latent heat of condensation from the permeate stream to preheat the feed stream reduces the thermal energy requirement in SWMD (Zhang et al. 2015). The thermal efficiency of the SWMD operation can be described by calculating the gained output ratio (GOR), which is the ratio of the heat associated with phase conversion to the heat being supplied to the system (Shahu and Thombre 2019).

3 Recent SWMD advancement

In order to push the SWMD application forward, the aforementioned operational challenges should be addressed. Major strategies during the SWMD operation and novel membrane fabrication have been extensively studied, and each of the studies corresponds to an effort to reduce one or more challenges, as presented in Figure 5.

3.1 Operational strategy

The alteration of operational conditions is mainly focused on the generation of a higher shear rate on the membrane surface, which can reduce both temperature polarization and concentration polarization, as well as fouling deposition (Figure 6). Several methods that have been conducted involved turbulence promoters and aeration (bubbling in feed input). From the operational side, the shear rate on the surface of the membrane can be increased by adjusting the fluid flow adjacent to the membrane in a turbulent regime. Martinez and Rodríguez–Maroto (2006) investigated the performance of DCMD modules with channel spacers and the concentration polarization was reduced by the addition of more spacers. Furthermore, it was noticed that the utilization of a coarse screen spacer reduced the temperature polarization and increased the permeate flux due to generated turbulence when fluid flowed through the spacer strands (Martinez and Rodriguez–Maroto 2007; Martinez–Diez and Vazquez–Gonzalez 1998).Computational studies on the effect of spacers on membrane performance were also performed and showed a similar result with the experimental studies. It was found that the temperature polarization decreased and the heat transfer rate increased when the spacer was inserted (Cipollina et al. 2009). Phattaranawik et al. observed a high flux enhancement of 31–41% when the spacers were set at hydrodynamic angles in the range of 70–90° and voidages of 60–70% (Phattaranawik et al. 2001). Despite the advantages, spacer increases the pressure drop across the channel and therefore led to inferior performance (Albeirutty et al. 2018). To evaluate the MD performance with different types of commercial spacers and different hydraulic diameters, Hagedorn et al. (2017) proposed a combined pressure drop and heat transfer correlation. The experiments indicated that thicker spacer resulted in better performance with lowest pressure drop of 0.037 bar/m and highest heat transfer coefficient of 5087 W/m^2 K. In the submerged configuration, transverse vibration of the membrane module was conducted to improve the shear rate on the membrane surface, as the control of the fluid hydrodynamic was rather limited (Kola et al. 2012). Molecular diffusion resistance in the membrane pores due to the presence of air was also identified as the limiting factor of vapor transport. Air removal using deaerated feed water was studied and higher flux was obtained at reduced O_2 saturation on the feed water. The thermal energy consumption of the module was reduced due to the elimination of conduction heat transfer (Winter et al. 2012).

Other studies were conducted using feed aeration in VMD configurations by mixing the hot feed solution and air in the inlet of the membrane module to form a gas/liquid two-phase flow in the membrane lumen. Using the polyvinylidene fluoride (PVDF) membrane, it was found that the permeate flux of feed-aerated test (60 L/h airflow rate) was twice as high as in the conventional VMD operation. This produced a significant reduction of temperature polarization and concentration polarization in

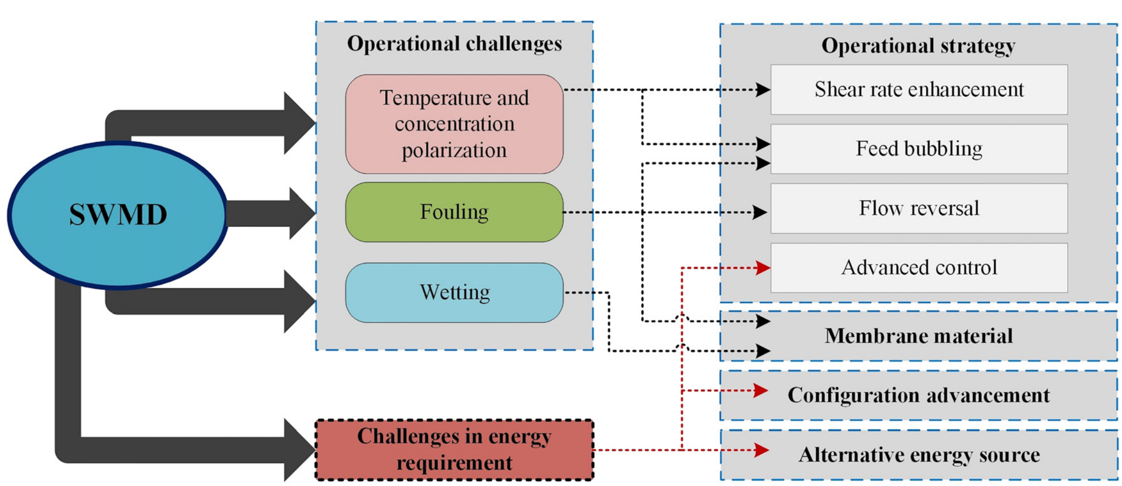

Figure 5: SWMD operation: major challenges and recent advancements.

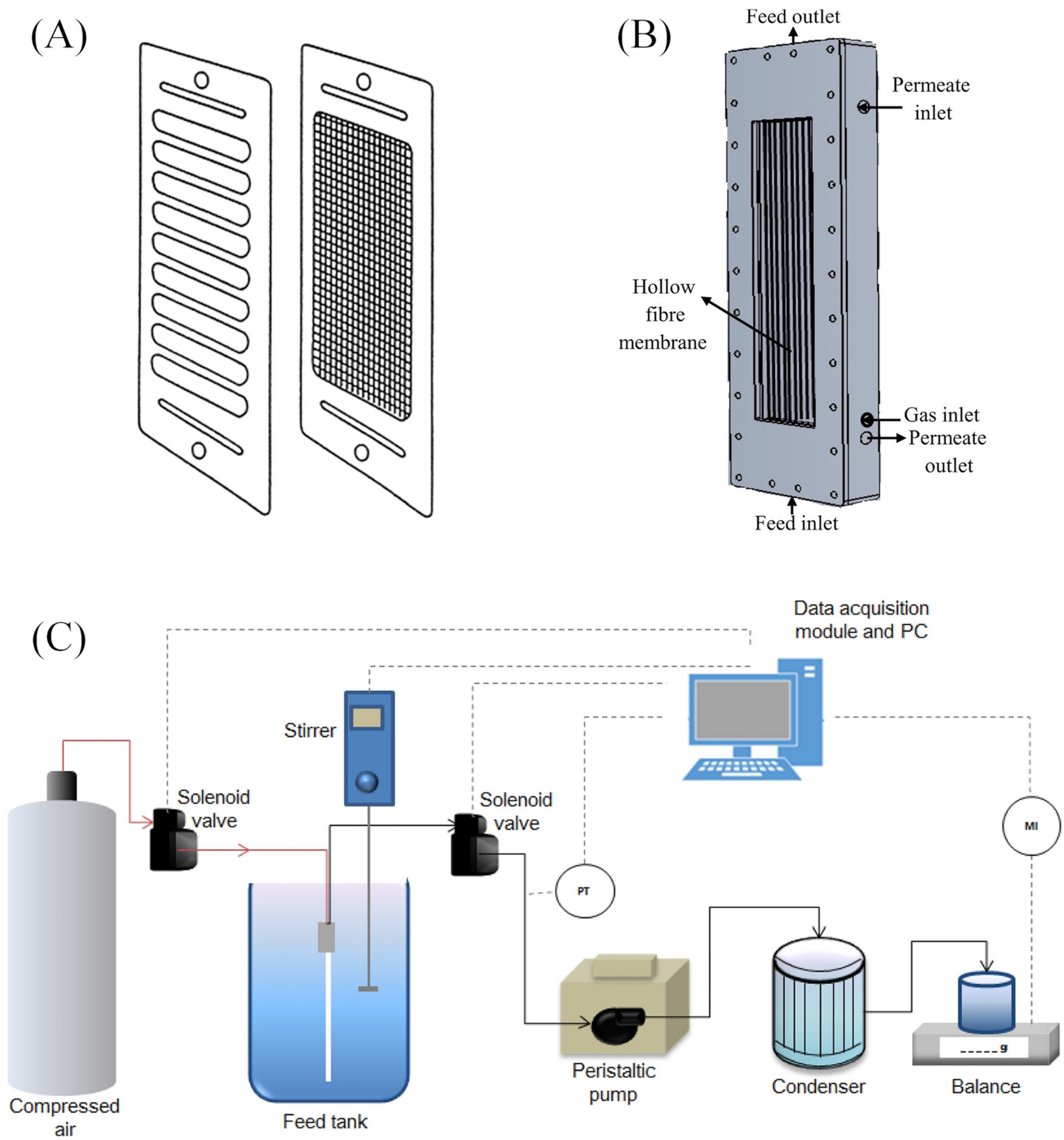

Figure 6: Operational strategies to improve MD performance. (A) Spacers (Martinez–Diez and Vazquez–Gonzalez 1998), reproduced with permission from Elsevier. (B) Air-bubbling (Chen et al. 2014), reproduced with permission from Elsevier. (C) Air-backwash (Julian et al. 2018), reproduced with permission from Elsevier.

the bubble-induced secondary flow and increased the superficial crossflow velocity. In addition, the flux decline of the test with feed aeration was much slower, as salt crystallization on the membrane surface was delayed due to the shear force generated by air-bubbling (Chunrui et al. 2011). However, it is important to note that the effectiveness of air-bubbling in enhancing MD performance is greatly influenced by the bubble size. Direct observation in DCMD applications for brine concentration confirmed that a higher shear rate and more even flow distribution could be created with fine bubbles in a narrow size distribution (Chen et al. 2014). In addition, the generation of bubbles in the feed solution delayed scale formation in the desalination operation because the liquid-gas interphase acted as a competitive nucleation site for heterogeneous nucleation, shifting the crystal formation on the membrane surface to the bulk feed solution (Julian et al. 2016). While these methods were able to increase the permeate flux and delay fouling formation, they were only effective in addressing external fouling. One of the strategies to overcome internal fouling is by performing a periodic air-backwash, in which pressurized air passes through the membrane in the opposite direction of the MD operation (Choo and Stensel 1998; Julian et al. 2018; Rattananurak et al. 2014; Stavrakakis et al. 2018).

MD performance can be enhanced by delaying nucleation of salt on the membrane surface which promotes scaling. Nghien and Cath conducted regular membrane flushing by Milli-Q water every 20 h of DCMD operation. Despite the high scaling tendency of $CaSO_4$ in the feed solution, extended operation time with stable permeate flux could be achieved due to the removal of the formed nuclei prior to rapid crystal growth (Nghiem and Cath 2011). Other studies reported temperature and flow reversal techniques to disrupt the nucleation of salt crystals on the membrane surface. The flow reversal method was carried out by reversing the feed side and permeate side after a predetermined period of operation time. As the permeate stream flowed in the feed compartment and the feed stream flowed in the permeate compartment, it was crucial to conduct a deep cleaning on both compartments between the flow reversals to maintain good permeate quality. While in temperature reversal mode, the temperature of the circulated feed was reduced so it was lower than that on the permeate side. Despite its simplicity, no further investigation of the crystallization mechanism was discussed in this study (Hickenbottom and Cath 2014). Wetting mitigation using a blower to drain the distillate in an AGMD module was studied in a long-term experiment. While the introduction of low pressurized air into the air gap channel resulted in slightly reduced flux and GOR, the permeate conductivity was significantly lower than the test without the air sparging, particularly at feed conductivity of more than 200 mS/cm (Schwantes et al. 2018).

Advanced control of MD operation has drawn much interest and been proved as a reliable tool to optimize MD performance. In a solar MD facility in Spain, a feedback control system was set and managed to reduce the settling time (i.e., time needed to establish the operating temperature of the MD). Also, the control system and the corresponding studied model were able to determine the optimum operating temperature at the inlet of the MD module (Gil et al. 2018b). The intermittent availability of solar energy results in the need for dynamic optimum operation conditions, which are challenging to be set manually. A hierarchical control system consisted of nonlinear model predictive control (NMPC) scheme and a direct control system was developed to automatically control the process variable. The system could optimize the distillate production, energy efficiency and cost-saving simultaneously (Gil et al. 2018a). In another study of solar MD utilizing indirect solar heat to attain stable solar radiation through the day and night, 10 design parameters were investigated to determine the minimum total annual cost (TAC) of the desalination plant. The minimum TAC was \$280,000 at the solar intensity of 500 W/m^2. The application of the control system resulted in stable permeate production, regardless of the daily weather (Chen et al. 2012).

3.2 Configuration advancement

There are four basic configurations of the MD process: DCMD, AGMD, sweep gas membrane distillation (SGMD), and VMD. The hot feed solution is continuously circulated and in direct contact with the membrane surface in all configurations. The distinction of each configuration is determined by the water vapor pressure condition between the feed and permeate stream (Phattaranawik et al. 2003). In DCMD, the cold permeate stream is circulated and in direct contact with the hot feed at the opposite membrane side. The temperature difference between the hot feed solution and the cold permeate stream creates vapor pressure difference and induces water vapor transport from the feed side to the permeate side (Ashoor et al. 2016). In AGMD, a stagnant air gap exists between the membrane and a cool condensing plate. The water vapor from the feed solution needs to pass across the air gap before being condensed at the surface of the condensing plate (Karbasi et al. 2017). In VMD, vacuum pressure was applied to the permeate side to create the vapor pressure difference. The water vapor travels across the membrane and condensed outside the membrane module (Mericq et al. 2010).

DCMD configuration is the most popular with more than 60% of MD studies carried out using a DCMD system (Khayet 2011), as it requires a simple configuration that possesses a high GOR (Summers et al. 2012). However, due to the continuous contact between the feed side and permeate side, high thermal polarization and relatively large conductive heat losses are inevitable (Fan and Peng 2012; Lawson and Lloyd 1996). In AGMD, heat losses are reduced and the energy efficiency is increased compared to the DCMD configuration (Summers et al. 2012). Even though mass resistance is high and relatively low permeate flux is expected, AGMD is more popular in commercial applications because of its high energy efficiency and capability for latent heat recovery (Patil and Shirsat 2017). In SGMD, lower thermal polarization and elimination of wetting on the permeate side were observed. However, SGMD is the least explored configuration due to the requirement of an external condenser (Zou et al. 2018). The VMD configuration provides higher permeate flux, lower thermal polarization, and negligible conductive heat loss as the vacuum is applied. However, it is highly prone to wetting and fouling (Drioli et al. 2015; Izquierdo-Gil and Jonsson 2003). An integrated DCMD–AGMD has been investigated, in which the feed exiting from the DCMD module was sent as a coolant stream in the AGMD module and was heated by the permeating vapor before being recycled back to the DCMD unit. The integrated system can be operated at higher temperatures (e.g., 50–60 °C for the DCMD and 70–80 °C for the AGMD). When compared to the single DCMD units, the integrated DCMD–AGMD systems has lower STEC (1.21–1.25 W/g/h), higher GOR (0.49–0.51), and higher permeate production (84.6–118.8 g/h) (Criscuoli 2016).

To further increase the permeation flux and energy efficiency, and to reduce the process footprint, the modification of the SWMD configuration is crucial (Table 1). This is directly related to the reduction of mass and heat transfer resistance as well as heat loss. Recently, a modification of the AGMD configuration was made by replacing air with another filling material (material gap membrane distillation [MGMD]) to reduce the mass transfer resistance and give a high salt rejection of 99.99% (Francis et al. 2013). Employing the appropriate filling material with low conductivity such as water and sand, a nearly five-fold increase in the transmembrane flux was achieved in the test using a PTFE flat sheet membrane for red seawater desalination (Francis et al. 2013).

To overcome low permeate flux and higher heat loss in AGMD and DCMD, some studies proposed liquid-gap membrane distillation (LGMD). In this configuration, the filling material was replaced by a liquid. A higher permeate flux was achieved than that of AGMD under the same operating conditions (Im et al. 2018). Contrary to the conventional wisdom regarding MD development, Ma et al. inserted a high conductivity material to the gap of the AGMD, creating conductive gap membrane distillation (CGMD). While a higher sensible heat loss is observed in CGMD, in the system utilizing cold seawater as the coolant, the heat can be readily transferred to the cold stream and preheat it, resulting in higher overall energy efficiency (Swaminathan et al. 2016). Some studies proposed a permeate-gap membrane distillation (PGMD) configuration, in which the water and volatiles components evaporate at the membrane interfacial surface of the evaporator channel. Compared to the AGMD, PGMD configuration provides an increase in the internal heat recovery, thus resulted in the increase of flux and GOR (Cheng et al. 2018).

Modification of the MD module using a multistage membrane distillation (MSMD) operation is also of interest (Figure 7). In the MSMD configuration, the latent heat released during the condensation of the permeate is used to preheat the cold feed water to achieve a high-performance ratio (PR), which is defined as the quotient of the amount of latent heat needed for evaporation of the water divided by the amount of heat provided to the system from an external energy source (Guillen–Burrieza et al. 2011; Khalifa et al. 2017; Lee et al. 2016; Liu et al. 2012). One modification with similar functional principles to the MEMD is multi effect vacuum membrane distillation (MEVMD) (Kiefer et al. 2018). At large-scale facilities, the latent heat energy is often recovered in an external heat recovery device, resulting in investment cost and electrical consumption enhancement. To improve the energy efficiency, DCMD can be integrated with a heat exchanger (HX) which recovers the latent heat in the permeate stream and use the heat to preheat the feed stream (Figure 7). This configuration reduces the energy requirement in the heater and cooler, hence results in improved GOR of the system (Chung et al. 2014; Guan et al. 2015). The concept of heat integration is vital to reduce energy consumption and operational cost; however, attention to the utilization of a low-cost heat exchanger is crucial. Another configuration is vacuum-enhanced DCMD (VE-DCMD) which results in a higher driving force by incorporating a vacuum on the permeate side (Alklaibi and Lior 2006; Naidu et al. 2017; Plattner et al. 2017).

Several commercial MD technology providers are still growing their business, promoting their technology, and leading the market. Aquastill, a company based in the Netherlands, become an MD technology promoter and holder of Memstill membrane distillation technology license (Thomas et al. 2017). Aquastill has also developed multi envelope spiral wound modules based on AGMD configuration that has been tested in a solar-powered MD at Plataforma Solar de Almería (Ruiz–Aguirre et al. 2017). Scarab focuses on technology that can be applied for desalination of seawater and RO brine in Sweden. It developed the heat recovery-AGMD module with a plate and frame heat exchanger designs with condensation plates (Wang and Chung 2015). Pilot plants were built in Sweden with Scarab modules in cascade configuration for water purification in a thermal cogeneration plant with a total production of 1–2 m^3/day of distillate (Zaragoza 2018). As the hollow fiber VMD developer, KMX Membrane Technologies (Canada) acted as technology developer for Bluestill membrane distillation technology (Macedonio and Drioli 2019; Zaragoza 2018). Memsift (Singapore) is continuing to explore other markets for its proprietary thermal separation process and membranes. Following an agreement formed earlier in 2020 with a Chinese company, a jointly developed brine treatment ZLD technology was set (Atkinson 2020). However, these commercial modules have not been tested for ZLD SWMD application, at which the modules capability to handle highly concentrated

Table 1: Studies of novel MD configurations.

Configuration	Material	Modification	Operation condition dan remarks	References
ME-VMD	PTFE	Combining two ME-VMD systems	Maximum GOR = 12.1 at feed temperature feed = 90 °C	Zhang et al. (2017)
	PP	Four stages VMD	Flux = 7 LMH	Zhao et al. (2013)
	PTFE	Adding supporting loops, such as heating, cooling, feed water, distillate, brine, and vacuum	Permeate flux = 50 L/h at feed temperature = 80 °C STEC = 300–700 kWh/m^3 GOR = 1–2.2	Mohamed et al. (2017)
V-DCMD	PTFE	Addition of vacuum pressure on the permeate side	Feed temperature = 55 °C Rejection = 96–99% Permeate flux increase by 42–67%	Plattner et al. (2017)
		Addition of vacuum pressure on the permeate side with water flushing	Feed temperature = 55 °C and permeate pressure = 300 mbar flux = 16.0 ± 0.3 L m^{-2} h^{-1}	Naidu et al. (2017)
MGMD	PTFE	Material gap filling (polyurethane, PP mesh, sand, and DI water) between the membrane and the condensation plate in an AGMD	Flux = 20.45 kg/m^2 h (428% increase) Material filling = water Feed temperature = 80 °C Coolant inlet temperatures = 20 °C	Francis et al. (2013)
CGMD	PTFE	Conductive spacer in the gap between the membrane and condensing surface	CGMD can have two times higher GOR than even PGMD. 40% higher GOR achieved when using counter-current flow	Swaminathan et al. (2016)
Multistage (MS)-VMD	PVDF	Multistage VMD with feed pump inlet, preheater, external brine heater, subsequent module which has vacuum side, vacuum pump	First stage's saturation temperature, T_{stage} (1) = 77 °C Last stage's saturation temperature, T_{stage} (N) = 35 °C MSVMD systems can be as efficient as a conventional MSF system.	Chung et al. (2016)
	PTFE with PP support	Utilizing waste heat contained in the thermal brine to raise the temperature of the feed	Feed temperature = 70 °C. Permeate temperature = 30 °C. Flux was reduced by 8%	Kayvani et al. (2016)
Multistage (MS)-AGMD and multistage (MS)-WGMD	PTFE	MS-AGMD and WGMD system Every single stage has a coolant chamber, condensation plate	Flux with 15% on average for MS-WGMD and 10% on average for MS-AGMD	Khalifa and Alawad (2018)
MS-AGMD	PTFE	Three identical AGMD modules	Feed salinity of 0.15 g/L The feed temperature = 70 °C The GOR reached 0.6 for parallel MS-AGMD system and 0.45 for the series MS-AGMD system	(Khalifa et al. 2017)
V-AGMD	PTFE	Develop vacuum pump (vacuum pressure 0.005–0.01 MPa) to eliminate the disadvantage of the air gap on membrane module (removal of noncondensable gases between the membrane and condensation tube surfaces)	Feed inlet temperature 40–80 °C; cross flow velocities of 0.039, 0.078, 0.116, and 0.155 m/s; salt concentrations (253, 2441, 6465, 16,335, and 44,825 ppm) Permeate flux 10.55 kg/(m^2 h) And thermal efficiency 62.82% at feed temperature 80 °C, flow rate 4 l/min and salt concentration 253 ppm	Abu-zeid et al. (2016)
V-AGMD	Low-density polyethylene (LDPE)	A pilot scale using two commercial spiral-wound modules at Plataforma solar de Almeria's solar desalination test	Flux permeate 8.7 l $m^{-2}h^{-1}$ for 1.5 m channel length module (membrane surface area 7.2 m^2), and energy efficiency 49 kW h GOR 13.5 for 2.7 m module (membrane surface area 25.9 m^2) These are the best experimental performances obtained so far with pilot scale modules in membrane distillation	Andrés-Mañas et al. (2020)

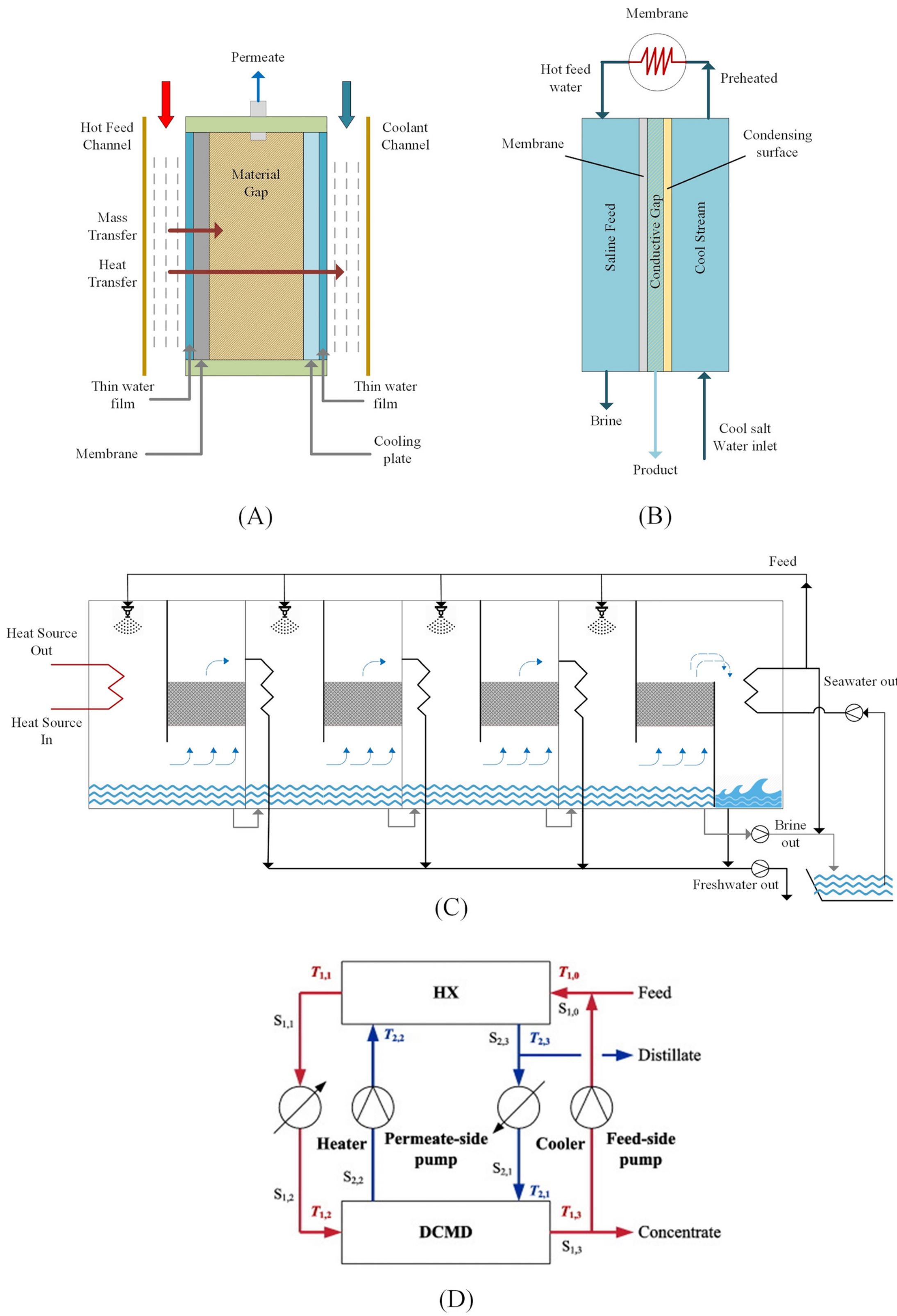

Figure 7: Schematic diagram of recent and modified MD, also configuration of (A) MGMD (Francis et al. 2013), reproduced with permission from Elsevier; (B) CGMD (Swaminathan et al. 2016), reproduced with permission from Elsevier; (C) MEMD (Christ et al. 2014), reproduced with permission from Elsevier; and (D) Schematic diagram of direct contact membrane distillation desalination system with heat recovery unit (Guan et al. 2015), reproduced with permission from Elsevier.

solution is crucial. In addition, to achieve ZLD operation, integration of the commercial membrane module with crystallizer is necessary.

Recently, vacuum-enhanced air-gap configuration (V-AGMD) was explored in a pilot-scale SWMD plant. In this configuration, a low-level vacuum was applied to remove air from the gap, reducing the mass transfer resistance. In oppose to the VMD, the vapor is condensed inside the gap in V-AGMD configuration (Abu–zeid et al. 2016; Andrés–manas et al. 2020). An improvement in permeate flux of up to 8.7 L m^{-2} h^{-1} was observed, which is significantly higher than the common AGMD configuration. The reduction of specific energy consumption and a GOR of 13.5 were also observed, confirming this study as the best SWMD operation on the pilot scale (Andres–manas et al. 2020).

3.3 Alternative energy source

Process improvement to reduce the energy requirements was conducted using solar thermal energy, particularly for applications in remote, arid areas, which normally require small-scale desalination systems. The combination of solar and fossil fuel desalination, as well as desalination using low-grade waste heat, could be more cost-effective under these particular conditions (Li et al. 2013). A comparison of solar-powered and fossil-powered SWMD plants was made using plate and frame MD technology. At a 100 m^3/day production rate, the fossil-powered SWMD plant showed a lower water production cost compared to that of the solar-powered plant (i.e. €7.19/m^3–€10/m^3). This could be due to the significantly higher capital, maintenance, and operation costs of the solar field. Interestingly, at relatively low water-production capacity, the solar-MD plant is already competitive with photovoltaic (PV)-RO (Ullah and Rasul 2019). By using solar collectors, which to heat the feed seawater before it enters the membrane module, high fluxes of 140 L h^{-1} m^{-2} were reached at a feed temperature of 70 °C. Based on this proposed design, an MD setup in Tunisia was built (Mericq et al. 2011). A VMD and a solar flat-plate collector (FPC) contributed to achieve a GOR of above 0.7, which was comparable to a simple-effect single-stage membrane distillation system (Ma et al. 2018).

Using an Aquaver WTS-40A prototype vacuum-multi effect membrane-distillation (V-MEMD), SEC values of below 200 kWh/m^3 could be achieved (Zaragoza et al. 2014). An onsite ZLD for brine water treatment, involving a brine-concentrator, membrane separator, and salt crystallizer was operated with 90% water recovery. The total energy requirement of this process was 91 kW h/m^3 with the annualized capital expenditure (CAPEX) and operational expenditure (OPEX) of \$0.305/m^3 and \$42.5/m^3, respectively (Alnouri et al. 2018). Another study using solar energy as the thermal energy source was conducted to evaluate the V-MEMD Memsys-module pilot performance. Mediterranean seawater was used as the feed solution and the feed was minimally pretreated by beach well filtration. To increase energy efficiency, a condenser acted as a heat recovery device, exchanging the latent heat of the distillate vapor with the feed seawater, which was used as a coolant. At optimum operation conditions (feed flow rate of 150 L/h and hot feed temperature of 75 °C), the maximum distillation flux was 8.5 L m^{-2} h^{-1}. The potential increase in productivity of SWMD using this particular configuration was limited by the cooling capacity of the system. In addition, scaling occurred after several months of operation, and the addition of an antiscalant to the feed was necessary (Andrés-mañas et al. 2018).

Banat et al. (2007b) conducted the SMADES project, which had two major components, a 72 m^2 collector field of flat-plate single-glassed collectors with absorbers made from standard copper pipes (Fenis, Turkey) and a 3 m^3 storage tank. This configuration required an SEC in the range of 200–300 kWh/m^3 and production cost \$15/m^3 for a 100 L/day water production (Banat and Jwaied 2008). Guillén-Burrieza et al. (2011) have reported the operational experience from three different types of air gap MD modules prepared and tested under the framework of the European project MEDESOL, aimed at investigation of solar-driven desalination. The maximum thermal energy observed was 79%, corresponding to an SEC of 810 kW h/m^3. A modeling study on solar MD was also presented by Chen and Ho (2010) using DCMD equipped with a solar absorber designed for saline water desalination and also by a pilot plant (evaluated by Memstill) with a freshwater production capacity of about 100 m^3/day (Dotremont et al. 2010). For the design of a solar-powered desalination system using MD in a remote area, energy efficiency is very important, since the investment costs mainly depend on the area of solar collectors to be installed, and the system design has to focus on very good heat recovery. A system using internal heat recovery resulted in an SEC of 100–200 kW h/m^3 distillate and a GOR of 3–6 when operating at 60–85 °C (Koschikowski et al. 2009). Another MD system with internal heat recovery was studied by Koschikowski with an SEC of 140–200 kW h/m^3 (Koschikowski et al. 2003). In a recent study, a pilot-scale V-AGMD using Aquastill commercial spiral-wound membranes was tested in Plataforma Solar de Almería's solar desalination facilities. Due to the fact that vacuum generation consumes a significant amount of energy, the traditional vacuum pump was eliminated, and the air in the module was extracted by means of the Venturi effect, due to the presence of a narrowing tube in the cooling flow circulation. A high-concentration feed in the range of 35.1–292.2 g L^{-1} was prepared; however, NaCl was the only feed constituent. The operation was conducted at two extremes: (i) extreme permeate productivity of 8.7 L m^{-2} h^{-1} and (ii) extreme energy efficiency with an STEC of 49 kW h/m^3. This operation showed a 68% reduction in STEC and was claimed as the best performance of pilot-scale MD to date (Andrés-mañas et al. 2020).

Most of solar MD has been operated by using spiral would modules with specific permeate channel due to the low electrical consumption and better internal heat recovery (Zaragoza 2018). However, solar energy is not available continuously and this affected the productivity and operational period of the solar MD system. Hence, it is important to optimize the size of the module and the control system to achieve better utilization of solar irradiation (Gopi et al. 2019). Geothermal energy is an abundant heat source and has the potential to support SWMD by utilizing alternative heat sources other than solar energy. SWMD is a more suitable technology to exploit geothermal energy for desalination than RO due to the low-grade heat characteristic of geothermal energy and the necessity to convert heat input into electric input that renders a lot of energy losses (Ali et al. 2018). Although AGMD or DCMD were suggested instead of VMD to avoid pore wetting (Jaafar and Sarbatly 2015), Sarbatly et al. presented the energy evaluation and analyzed the application of VMD for the treatment of geothermal water by the geothermal heat source. Compared to the plant without geothermal energy utilization, the water production costs of the plant operated with geothermal energy was less than \$0.50/m^3 (Sarbatly and Chiam 2013). Geothermal energy is expected to reduce the cost of water production; however, the application of this energy is still new for membrane distillation.

3.4 Membrane material

The modification of membrane material is an effort to engineer the membrane properties and characteristics to produce a specifically-designed membrane suitable for a particular application. The choice of membrane material for SWMD is crucial, as it dramatically influences separation performance. As for now, no commercially available membrane is specifically designed for MD operation. Pilot-scale SWMD operated worldwide use polymer-based membranes, such as polypropylene (PP), polyethylene (PE), PVDF, or polytetrafluroethylene (PTFE) (Kujawa 2019), with MF-like pore size. Though some research has investigated the application of inorganic membrane for SWMD applications, membrane cost has become a major drawback for its industrialization. This is particularly true, as the SWMD application is not operated at extremely high temperatures (Hubadillah et al. 2019). In terms of membrane structure, pore size, porosity, thickness, and tortuosity of the membrane are important parameters that determine the permeate flux of MD (Chen et al. 2017; Dizge et al. 2019). In general, the membrane with high porosity and low tortuosity is preferred, as it promotes high flux (Khayet et al. 2005). The increase in flux can also be obtained with bigger pores, yet this might promote more severe scaling and wetting at high salt concentrations in the feed (Tijing et al. 2016). While heat transfer through conduction is considered a parasitic heat loss that reduces the energy efficiency and permeate flux of MD operation, relatively thick membranes are often used in SWMD (Chen et al. 2018). However, a thick membrane leads to high mass transfer resistance, inhibiting vapor transport in membrane pores. Hence, the optimization of pore size and membrane-thickness are necessary. In the recent development of membrane fabrication, the application of green solvent to replace the commonly used organic solvent is also of interest. The green solvent is more environmentally friendly and does not pose a threat to human health. Fabrication of PVDF hollow fiber membrane for DCMD has been conducted by phase inversion using triethyl phosphate (TEP) as the solvent to replace the commonly used N-Methyl-2- pyrrolidone (NMP). The fabricated membrane exhibited a flux of 20 kg/m^2 h and NaCl rejection of 99.99% with robust mechanical properties and high liquid entry pressure (Chang et al. 2017).

Another important parameter in selecting the membrane material for the SWMD application is the material hydrophobicity. Research in membrane materials focuses on superhydrophobic materials, which can overcome fouling and wetting problems. Superhydrophobic material with a contact angle of more than 150° reduces fouling deposition by increasing the surface roughness and having low surface energy (Dizge et al. 2019; Ragunath et al. 2018; Zhang et al. 2014). Methods to achieve superhydrophobic are many: dip coating, vacuum coating, surface functionalization, plasma treatment and many more, and have been extensively reviewed (Bernardes et al. 2014; Chen et al. 2017; Hubadillah et al. 2019; Khan et al. 2019; Ma et al. 2001). Table 2 presents recent selected studies in material modification for the SWMD application. Most studies focus on the fabrication of nanocomposite membranes using nanoparticles (such as silica, titanium dioxide [TiO_2], graphene oxide [GO], and carbon nanotubes [CNT]) blended in a dope solution or coated onto the support-polymer membrane. Functionalization of the nanoparticles

Table 2: Recent advances in superhydrophobic membrane fabrication.

Membrane type	Material	Modification/treatment	Remarks	References
Nanocomposites	Polymer: Polyether sulfone (PES); inorganic: nanosilica	Vacuum filtration coating with perfluorodecyltryethoxysilane (FDTES) and polydimethylsiloxane (PDMS)	Better permeate flux, salt rejection, and antifouling properties at test using 1M NaCl and 10 mg/L HA than PP and PVDF membrane	Khan et al. (2019)
Nanocomposites	Polymer: PVDF; inorganic: TiO_2	Coating with TiO_2 solution and fluorination of TiO_2-PVDF membrane	Slightly reduced permeate flux of the modified membrane, with better antifouling performance in test using 150 g/L HA and 3.77 mM $CaCl_2$	Razmjou et al. (2012)
Nanocomposites	Polymer: PP; inorganic: Silica	Coating with silica following modification with 1H,1H,2H,2H-Perfluorooctyltriethoxysilane (POTS)	High contact angle of 157°, higher flux, and salt rejection in test using 3.5 wt. % NaCl	Xu et al. (2017)
Nanocomposites	Polymer: PVDF inorganic: Silica	Aminosilane functionalization and silica nanoparticle grafting	Omniphobic membrane, good performance for desalination of challenging industrial wastewater. However, lower flux than virgin membrane was obtained	Boo et al. (2016)
Nanocomposites	Polymer: PVDF; inorganic: Silica	Forming perfluorooctyl trichlorosilane (PFTS) and coating silica (SiO_2) nanoparticles onto the membrane surface	Better fouling performance in test using NaCl solution (3.5 wt. %), kerosene, SDBS, and HA to mimic the seawater	Lu et al. (2016)
Nanocomposites	Polymer: PVDF; inorganic: Hyflon AD	Original PVDF membrane was dipped in (dip-coating) in Hyflon AD solution	The composite membranes showed enhanced fouling and wetting resistance and maintained stable salt rejections	Li et al. (2019)
Nanocomposites	Polymer: PVDF; inorganic: Reduced-graphene oxide (rGO)	Phase inversion of PVDF–rGO blend	Stable flux with no wetting for up to 96 h of operation, higher permeate flux compared to the pristine PVDF membrane without compromising the salt rejection	Abdel-Karim et al. (2019)
Nanocomposites	Polymer PP (support) and PVDF (selective layer); inorganic: CNT	Coating of PVDF–CNT mixture on the polypropylene surface	The water vapor flux by CNIM membrane was as high as 51.4 L m^{-2} h^{-1}, which was 76% higher than the unmodified support membrane at 60 °C. No significant salt leakage was observed with modified membrane	Ragunath et al. (2018)
Nanocomposites	Polymer: PVDF; inorganic: functionalized-GO	GO was functionalized with 3-(aminopropyl)triethoxysilane (APTS), followed by dissolving PVDF and GO in dimethyl formamide (DMF) before casting	In the AGMD test using 3.5 wt. % NaCl as the feed solution, flux of 6.2 L m^{-2} $h^{-1}$and 99.9% salt rejection was obtained	Leaper et al. (2018)
Nanocomposites	Polymer: PVDF; inorganic: GO-NBA (n-butylamine modified graphene oxide)	Dope preparation by adding GO fine powders into PVDF. Polymer mixing and phase inversion	Greater mechanical properties than that of conventional GO because of better compatibility, dispersity, and crystalline structure. Flux was 61.9 L m^{-2} h^{-1} and a salt rejection was 99.9% at the test with seawater feed	Lu et al. (2017)
Electrospun	PVA and silica nanoparticle	Electrospinning of PVA–SiNPs blend, followed by calcination and fluorination	Superamphiphobic MD membranes with antisurfactant-wetting, robust in feed containing SDS	Huang et al. (2017a, b)
Electrospun	Polysulfone (PSf) and fluorinated polyurethane additive (FPA)	Electrospinning to produce ultrathin fiber polymer	Competitive permeate flux as high as 53.8 L m^{-2} h^{-1}, with stable low, permeate conductivities in a test using 30 g/L NaCl solution (35 h)	Khayet et al. (2019)
Electrospun	Polymer: PVDF; inorganic: CNT	Electrospinning of PVDF dope solution, followed by spraying of CNT in ethanol	Highest water flux (28.4 L m^{-2} h^{-1}) with steadyVMD performance for more than 26 h. The feed solution was 3.5% NaCl solution	Yan et al. (2018)

Table 2: (continued)

Membrane type	Material	Modification/treatment	Remarks	References
Inorganic	GO, polydopamine (PDA)-modified-Al_2O_3	Vacuum filtration of GO slurry on top of PDA modified Al_2O_3 disk	For desalination of 3.5 wt. % seawater at 90 °C, high water flux of 48.4 L m^{-2} h^{-1} and high ion rejections of over 99.7% can be obtained	Xu et al. (2016)
Inorganic	Ceramic: Al_2O_3, TiO_2, ZrO_2	Ceramic membranes were modified in the grafting solution (0.05 M). Membrane modification was accomplished by soaking the sample in grafting solution (during 1.5 or 3 h) at room temperature.	Membranes were successfully modified, and no wetting (contact angle of up to 154°) was observed. Salt rejection of membrane was 99% and flux was in the range of 0.31–8.95 L $m^{-2}h^{-1}$	Kujawa (2019)
Polymer	PVDF, PDA	Membrane coated by $AgNO_3$ and conducted in an anhydrous ethanol solution containing 10 mM 1H, 1H, 2H, 2H-perfluorodecanethiol	Excellent antifouling capability was achieved when dealing with saline water composed of 35 g/L NaCl and 1.26 g/L $CaCl_2$	Shan et al. (2018)
Polymer	PTFE	Graphene film from a renewable source, such as soybean oil homogeneously coated the PTFE membrane	Wetting or fouling of the membrane surface was insignificant in the graphene-based membrane and salt rejection was 99.9%	Seo et al. (2018)
Polymer	PES	Dip-coating with silica nanoparticles, followed by vacuum filtration coating with 1H,1H,2H,2H-perfluorodecyl triethoxysilane and polydimethylsiloxane	The membrane showed no severe fouling and/or wetting for more than 15 and 25 h	Ahmad et al. (2019)
Polymer	PVDF	CF_4 plasma treatment	Higher permeate flux	Chen et al. (2017)

or further surface modification of the nanocomposite membrane was required to tailor the superhydrophobicity. Nanoparticles dispersed in the polymer created an additional self assembly layer on top of the polymer structure, forming a rougher surface and enhanced hydrophobicity. A high contact angle of 150°–157° was achieved (Xu et al. 2017), and the modified membrane exhibited excellent performance with a high flux of more than 50 L m h (Ragunath et al. 2018) and superior salt rejection. The fabrication of a nanocomposite electrospun membrane was also highlighted. Theoretically, electrospun membranes boast an interconnected pore structure with a shorter path for the diffusion of molecules, which allows higher flux to be obtained without compromising the membrane's mechanical integrity. In the electrospinning method, the inorganic phase could be dispersed into the polymer to form an organic–inorganic blend, or it could be sprayed onto the electrospun polymer surface (Yan et al. 2018). However, electrospinning is not economically feasible for membrane fabrication on a large scale.

In addition to superhydrophobic membranes, omniphobic membranes, which possess unique wettability characteristics, show great promise in membrane modification studies (Lu et al. 2019a). In particular, omniphobic membranes have been developed for MD applications involving liquids such as oils and organics as the feed. Omniphobic membranes decrease surface tension more than superhydrophobic membranes and can repel high and low-surface-tension liquids (Figure 8). The main features of omniphobic material are low-surface energy material and specific re entrant structure to maintain the Cassie–Baxter nonwetted state (Lu et al. 2018). The critical role of slippery omniphobic membrane in mitigating membrane scaling has been discussed recently. Slippery membrane hinders heterogeneous nucleation on the membrane surface and bulk crystal deposition due to its nonadhesive property. In a study comparing PVDF and omniphobic slippery modified PVDF (OMNI-SLIP), it was known that the Gibbs free energy for heterogeneous nucleation in OMNI-SLIP membrane was higher than the PVDF membrane due to the lower porosity and higher contact angle. This indicated higher energy barriers for heterogeneous nucleation. While homogeneous crystal formation may occur in the bulk feed solution, the slippery characteristic of the omniphobic membrane inhibited the deposition of the crystals on the membrane surface (Chen et al. 2020a).

The Janus membrane was developed to provide a high mass transfer without sacrificing the membrane's selectivity by integrating materials of opposing wettability. Through asymmetric fabrication or asymmetric decoration, hydrophobic and hydrophilic materials are bound

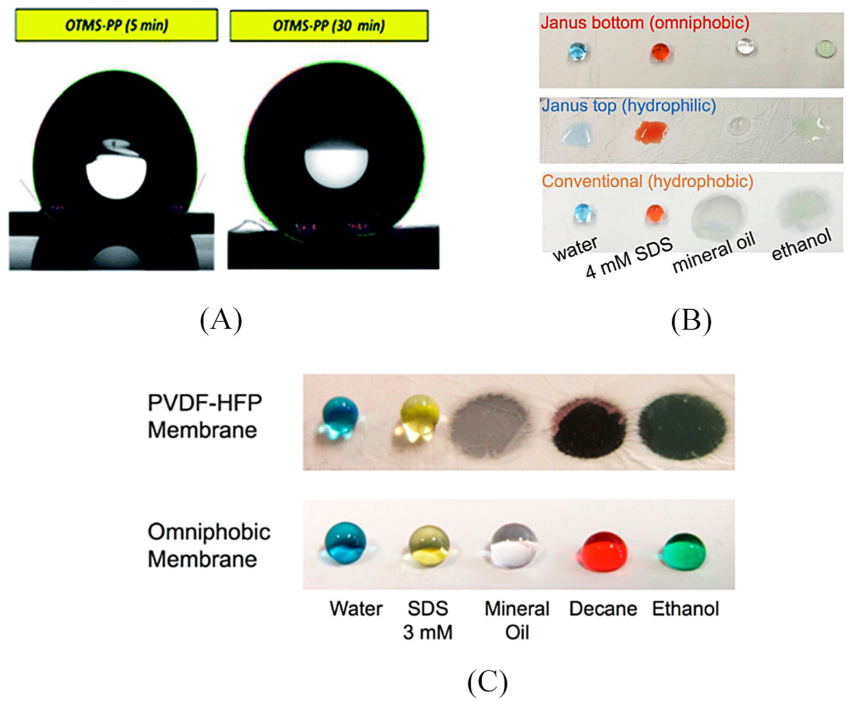

Figure 8: Contact angle of modified membrane (A) hydrophobic to superhydrophobic (octadecyltrimethoxysilane coated onto polypropylene surface) (Ray et al. 2018), published by the Royal Society of Chemistry; (B) hydrophobic to Janus (omniphobic–hydrophillic) membrane (Huang et al. 2017b), reprinted (adapted) with permission from (Huang et al. 2017b), copyright (2013) American Chemical Society; (C) hydrophobic to omniphobic membrane (electrospun poly(vinylidene fluoride-co-hexafluoropropylene) (PVDF-HFP) and benzyltriethylammonium. Negatively charged silica nanoparticles (SiNPs) were grafted via dip-coating) (Scaffold et al. 2016), reprinted (adapted) with permission from (Scaffold et al. 2016), copyright (2016) American Chemical Society.

together to form two layers, each facing the opposite side. The two layers may share similar thicknesses, yet in many modifications, one side is significantly thinner than the other. In a recent study, an ultrathin dense composite Janus membrane was fabricated following the layer-by-layer assembly method. The dense hydrophilic layer was consisted of polyethylamine (PEI) and polyanion poly (sodium 4-styrenesulfonate) (PSS) deposited interchangeably onto the PVDF substrate. In the test using a mixture of NaCl and SDS as the feed solution, the wetting resistance of the fabricated Janus membrane was improved due to the size exclusion mechanism. Therefore, the PEI/PSS layer rejected the SDS molecules while allowed the NaCl and water to pass through. The surface tension of the NaCl solution inside the multilayer structure is significantly higher than the initial feed solution, which resulted in alleviated wetting (Chen et al. 2020b). The omniphobic and Janus membranes for MD application exhibit higher flux and lower fouling tendencies due to the unique wettability properties (Yao et al. 2020). However, the fabrication of chemically and mechanically robust omniphobic and Janus membranes is still challenging, particularly for large scale hollow-fiber membranes.

While promising results were obtained with the modified membrane for the SWMD application, there were two concerning gaps that were noticed during the examination of modified membrane performance for the SWMD application; (1) The use of synthetic seawater as the feed solution in most experiments and (2) the relatively short operation time of the experiments. In most studies, synthetic seawater containing 3–3.5 wt. % of NaCl was used as the feed solution, with the addition of low concentration of organics, such as HA in a few tests (Khan et al. 2019). While NaCl is the highest concentration salt in seawater, severe scaling due to the single deposition of NaCl is extremely rare. This is due to the high solubility of NaCl in water (360 g/L at 25 °C) (Khadijah et al. 2018). Also, NaCl has a positive temperature-solubility coefficient; hence, its solubility increases with the enhancement of temperature, which is the case in an MD operation (Hubadillah et al. 2018; Luo et al. 2018). Scaling in MD mostly consists of sparingly soluble salts, such as $CaSO_4$ and $CaCO_3$, which pose a negative temperature-solubility coefficient. The presence of these sparingly soluble salts in the feed solution that is used to test the modified membrane may present interesting results and novel findings on how the modified membrane reacts to a rather complex feed solution. A separate issue is that the modified membranes were tested over a short operation time. While the superiority of the modified membrane over the nascent membrane was obvious during the short operation time, there is a dearth of studies focusing on the true robustness of the modified membrane. For SWMD operation to be economically feasible, long-term membrane stability, both mechanically and chemically, is a critical parameter.

4 Comparative study of SWMD and SWRO

The MD application for desalination has been applied for a high salt-concentration feed, such as inland brine water and produced water. Research on the application of MD for direct seawater desalination is limited, despite its potential. Many studies highlight MD's inability to economically compete with RO, particularly in terms of energy consumption, and suggest MD utilization as a complement to SWRO. At the seawater salt concentration, the energy to overcome the osmotic pressure of the feed is lower than that to increase the feed temperature as in the MD application. However, further research on SWMD has succeeded in reducing the operational cost. Also, other MD operational aspects (e.g. fouling characteristics and feed pretreatment) are potentially superior to SWRO.

4.1 Membrane fouling characteristics

The formation of a fouling layer, which is the deposition of unwanted solute on the membrane surface, should be delayed, as it increases the operating and maintenance cost of the seawater desalination process. In addition, fouling also reduces the quality and quantity of the produced permeate. While all types of fouling occur during SWRO and SWMD, the structure and severity of each fouling are significantly different. In SWRO, biofouling is considered as a serious threat and has become the main reason for flux decline in the SWRO plant in the Middle East. While the EPS only resulted in 2% flux decline, the presence of dead cells increased the flux decline percentage to up to 5–6% (Maddah and Chogle 2017). One of the potential causes of severe biofouling in SWRO is the operating temperature. SWRO plants, particularly in the Middle East, are operated at a temperature of approximately 35 °C. At such a temperature, the degradation of HA into smaller molecules that serve as nutrients for microorganisms is much easier than at lower temperatures. It was observed that the $1 million membrane inventory lasted only for half of its theoretical life-span due to biofouling, and this added $125,000 of cost per year (Flemming 1997).

Biofouling formation in SWMD is limited by the high operating temperature and the hydrophobicity of the membrane. The high operating temperature only allows the survival of thermophilic microorganisms (thermal effect). In a recent study, biofouling behavior in SWMD was investigated in concentrating and nonconcentrating modes. Experiments in the nonconcentrating mode focused on the influence of the thermal effect on the biofouling formation, and the results revealed three sequential phases of biofouling formation. Phase I marked the formation of a conditioning film consisting of suspended particles, colloids, dissolved organic foulants, and EPSs. In Phase II, a shift in the microbial community was observed, and the diversity of the microorganisms declined. However, the biofilm initiated and formed rapidly, indicated by a significant flux reduction. With biofilm formation and metabolism, some bacteria grew rapidly and secreted a particular type of EPS, making a thicker and more compact biofilm. Related to the severe temperature polarization due to biofilm formation, the EPS protected the microorganisms in the biofilm from the hot solution and lead to the growth of other microorganisms (Phase III). In concentrating mode, the effect of feed salinity enhancement on biofouling formation was studied, and the biofouling can also be divided into three phases. The first phase was similar to the nonconcentrating mode with the initialization of film formation. However, as feed salinity increased, initial scaling and biofouling were observed simultaneously in Phase II. In Phase III, severe scaling and biofilm were further developed and created a thicker and denser fouling layer compared to the nonconcentrating mode (Jiang et al. 2020).

Zodrow et al. (2014) compared bench-scale DCMD and RO with an identical seawater feed and investigated biofouling formation and structure. It is worth noting that during four days of operation time, a significant decline in microorganism concentration, dead cells, and EPSs in the MD system was observed. While both membranes in MD and RO operation suffered from biofouling, the total biovolume of biofilm in MD was lower than that in RO. In addition, the structure of biofilm differed greatly, with homogeneous biofilm and heterogeneous colonized biofilm being observed in RO and MD, respectively.

In contrast to biofouling formation, a high feed-temperature in SWMD has a detrimental effect on scale formation. As previously discussed in Section 2.2, scale in SWMD consists of negative temperature-solubility coefficient salts, whose solubility decline with an increase in temperature. As MD operates at elevated temperatures, the solubility of those sparingly soluble salts decreases, which exacerbates their precipitation. This is aggravated by the occurrence of concentration polarization, which indicates an elevated ion concentration on the feed-membrane interface. Temperature polarization might have the opposite effect on scale formation. At a lower feed-membrane temperature, the solubility of those salts should increase, yet its impact is insignificant and severe scaling is observed in most SWMD studies. Scaling in SWMD has been successfully limited by simple pretreatment, such as the addition of an antiscalant and the utilization of ultrafiltration (UF)/NF) (Drioli et al. 1999; Warsinger et al. 2015).

4.2 Seawater feed pre-treatment

Feed pretreatment is a critical step of all membrane-based seawater desalination processes. In general, the feed pretreatment aims to alter the seawater composition, directly effecting the potential fouling reduction. In SWRO operation, fouling resulted in more frequent membrane replacement, which accounted for 13% of total water production cost. The fouling management strategy should be chosen according to the characteristics of the seawater and the desired product. Impurities in the seawater consist of particulates, colloidals, inorganic compounds, water-borne microorganisms, and a small concentration of heavy metals. These impurities may result in particulate fouling, inorganic fouling, and biofouling. In SWRO operation, conventional pretreatment includes, but is not limited to coagulation/flocculation, granular media filtration, disinfection, and addition of a scale inhibitor or lime treatment. Other strategies, such as UV radiation and the application of dissolved-air flotation may also be conducted, depending on the initial quality of the seawater. Disinfection is performed to ensure 100% microorganism removal, which is essential, as the presence of a single microorganism can initiate biofouling due to the ability of the microorganisms to proliferate. Disinfection can be conducted by chlorination, ozonation, and ultrasound, where chlorination is the most prominent method. The addition of chlorine into the seawater raises another concern as the commercial RO membrane is made of polyimide which is highly susceptible to chlorine. Thus, complete chlorine removal is necessary before SWRO to avoid the detrimental impact on RO performance.

The possibility of failure during filter backwash and the poor removal of particles < 10 um is a major disadvantage of conventional seawater pretreatment for SWRO. This has led to the development of membrane-based SWRO pretreatment, utilizing mainly microfiltration (MF), UF, and NF. Using UF for the pretreatment of seawater with a total dissolved solids (TDS) of 40500 mg/L, the optimum water recovery rate in the range of 50–60% was obtained (Glueckstern et al. 2002). UF pretreatment also resulted in a negligible fouling rate during 30 days of RO operation of Mediterranean seawater (Lorain et al. 2007). Chemical usage in membrane-based pretreatment is significantly lower than that in conventional pretreatment. In conventional pretreatment, a significant number of chemicals are used in coagulation, flocculation, and as a biocide. This increases the operational costs for chemical supply and sludge treatment prior to discharge into the environment. In membrane-based pretreatment, chemicals are mainly used for membrane cleaning. However, a higher energy demand is obtained in membrane-based pretreatment, making it less environment friendly.

Even though studies have shown that MD is less susceptible to fouling and does not require extensive pretreatment (Alkhudhiri et al. 2012; Camacho et al. 2013), SWMD operation is susceptible to inorganic fouling. Thus, most of the feed pretreatment targets the removal of divalent ions, such as Ca^{2+} and Mg^{2+}. Gryta investigated thermal water softening to remove salts with negative solubility-temperature coefficient. By increasing the feed temperature for a certain period before the MD operation, the salts precipitated in the bulk solution and their concentration was reduced. Delayed flux decline was observed, signifying the potential of this method (Karakulski et al. 2002, 2006). However, a significant amount of energy was needed to maintain the high-temperature feed solution during the pretreatment. Analogous to RO, membrane technology has been considered one of the best resorts for feed pretreatment. In the path of ZLD SWMD, RO can also be categorized as a pretreatment of MD, separate from MF, UF, and NF. In a study of integrated membrane technology, MF/UF, RO and MD were operated subsequently to desalinate the feed solution with a concentration of 45 g/L. The recovery factor of RO was 40% and the RO retentate with a concentration of 75 g/L was further processed in the MD at 35 °C. The recovery factor of MD was 77% and the retentate concentration was 320 g/L. In this system, the overall water recovery of 87.6% could be achieved, significantly higher than SWRO alone (Drioli et al. 1999). In a recent study, the water recovery of the desalination process was enhanced by operating hybrid systems on the pilot scale, which were a combination of UF, NF, RO, chemical deposition, MD, and an antiscalant. The highest water recovery of 84.59% was obtained in the RO – MD system, with the addition of an antiscalant to the RO brine prior to the MD operation (Bindels et al. 2020). These findings highlight the ability of SWMD to be operated at an extremely high feed concentration, when SWRO is limited by the osmotic pressure (Mericq et al. 2010).

4.3 Energy requirement

The energy source of SWRO is electricity with SEEC ranged from 3.5 to 17 kW h/m^3. In SWMD application, as mentioned in Section 2.4, both electrical and thermal energy are applied simultaneously. Direct comparison of the energy requirement of the SWRO and SWMD, assuming equivalent grade of electricity energy and low-grade heat energy, is not entirely correct. Comparison of desalination processes using various energy inputs would need further analysis based on the approach to exergetic analysis and the second law of thermodynamics. The different energy input could be transformed into a common unit known as the standard primary energy (SPE) (Shahzad 2019). The SEEC, STEC, and SPE of selected SWMD and SWRO process are presented in Table 3. While the SEEC of SWMD plants is lower than for SWRO, the STEC is significantly high, particularly in

Table 3: Energy requirement of selected studies in SWMD and SWRO.

Configuration	Energy source	GOR	SEEC (kW h/m^3)	STEC (kW h/m^3)	Standard primary energy (kW h/m^3)	References
DCMD (pilot-scale tests)	Waste heat energy (low pressure steam and diesel heater)	10–17	–	38.61–64.16	1.09–1.82	Jansen et al. (2013)
AGMD (spiral-wound)	Thermal and electrical energy source	6.5–7	0.13	90	2.81	Duong et al. (2016)
V-MEMD	Solar energy as thermal source	3.2	5–20	200	15.72–45.90	Andrés–Manas et al. (2018)
AGMD (multichannel spiral-wound modules)	Solar field and heat exchanger	5.45	–	106.6	3.02	Ruiz–Aguirre et al. (2018)
Plate and frame MD	Solar energy using collector field	1.69	–	374.8	10.61	Guillén–Burrieza et al. (2015)
VMD	Solar thermal system	–	–	580	16.42	Joo and Kwak (2016)
AGMD	Solar energy, flat plate solar circuit	–	–	20	0.57	Asim et al. (2016)
V-AGMD (spiral wound Aquastill)	Solar energy	13.5	–	49	1.39	Andrés-Manas et al. (2020)
DCMD	Electricity	3.4 with HX	–	–	–	Chung et al. (2014)
SWRO	–	–	4.5–8.5	–	9.05–17.10	Eltawil et al. (2009)
SWRO	–	–	0.76	–	1.53	Gordon and Hui (2016)
SWRO (Fukuoka desalination plant, Japan, 50,000 m^3/day at maximum capacity)	N/A	–	5.0	–	10.06	Shimokawa (2009)
SWRO (Llobregat SWRO plant, Spain, 24.6 m^3/day)	N/A	–	4.17	–	8.39	Abdelrasoul et al. (2017)
SWRO (Soreq, Israel)	Double work exchanger energy recovery	–	2.7	–	5.43	Taylor and Efraty (2012)
Perth SWRO plant (capacity 28 m^3/day)	N/A	–	3.40	–	6.84	Abdelrasoul et al. (2017)
Tuas SWRO plant, Singapore (19.7–24.6 m^3/day)	N/A	–	4.35	–	8.75	Abdelrasoul et al. (2017)
SWRO (Hadera, Israel, 100 M m^3/year)	Electricity	–	2.7	–	5.43	Taylor et al. (2013), Kim and Hong (2018)
Askhelon SWRO plant (330,000 m^3/day)	Electricity (double work exchanger energy recovery)	–	3.0	–	6.04	Sauvet–Goichon (2007)
SWRO Fujairah plant (170,500 m^3/day)	Power plant (electricity)	–	3.7–3.9	–	7.44–7.85	Angel et al. (2006)
SWRO test site, affordable desalination collaboration (ADC), USA 200–300 m^3/day	N/A	–	1.58	–	3.18	Fritzmann et al. (2007)
Aqualyng SWRO plants (1000–5400 m^3/day)	Installation of exchanger isobaric chambers as energy recovery devices (ERD)		1.9–2.5		3.82–5.03	Fritzmann et al. (2007)

the absence of STEC in most SWRO plants. However, comparing the energy requirement of SWRO and SWMD in terms of SPE, it is clear that few MD operations required lower energy than SWRO.

4.4 Economic evaluation

The industrialization of SWMD greatly depends on economic evaluation and the water production cost, which is the sum of the capital cost (hardware, utility, and site preparation) and operational cost (electrical, heat source, maintenance, labor, and membrane replacement). In particular, SWMD should compete with SWRO as the desalination market leader to date with a water production cost of \$0.5–1.2/m^3 (Ismail et al. 2018). The hybrid RO + MD operation was investigated on a pilot scale and a techno-economic analysis was conducted. The RO brine was further treated in MD to increase the water recovery, as MD is capable of being operated at a high salt concentration, where RO is no longer economically feasible due to the extreme osmotic pressure. An antiscalant was needed to pre-treat the RO brine, thereby reducing the scaling problem in MD. In this study, the techno-economic analysis was conducted at a design capacity of 45,000 m^3/day with 90% uptime. The price of the MD module was interpolated from the pilot-scale Aquastill module and a total water cost of USD 0.63/m^3 was achieved. Another hybrid configuration involving RO + NF + MD was also studied. The RO brine was treated by NF and, subsequently, the NF brine was further concentrated in MD with the addition of an antiscalant. In this configuration, a total water recovery of 73.38% and a total water cost of USD 0.7/m^3 were obtained. However, it is important to note that this study assumed the availability of waste heat onsite for supplying the energy to the MD system (Table 4) (Bindels et al. 2020). This assumption is a critical determinant of the total water cost as the thermal energy requirement (STEC) in MD accounts for the vast majority of the total energy requirement (Table 3).

By using a cost-optimization model to assess the techno-economic feasibility of MD, it can be concluded

Table 4: Water production cost of various SWMD operations.

Membrane module	Configuration	Water recovery (%)	Capacity (m^3/day)	Heating source	Total water cost	References
Aquastill (pilot-scale)	RO-AGMD (with antiscalant)	RO = 50% MD = 69.18% Total = 84.59%	45,000	Waste heat	0.63 USD/m^3	Bindels et al. (2020)
	RO-NF-AGMD (with antiscalant)	RO = 50% NF = 30% MD = 77.92% Total = 73.38%			0.7 USD/m^3	
Memstill	AGMD	MD = 50%	10,5000	Fuel-fired Cogeneration Waste heat	0.54 USD/m^3 0.35 USD/m^3 0.31 USD/m^3	Meindersma et al. (2006)
Keppel Seghers	LGMD (three module)	–	100	Gas boiler	7.2 €/m^3	Guillén–Burrieza et al. (2015)
N/A	AGMD (parallel configuration)	–	Laboratory scale	Electricity	0.13 USD/L (>100 €/m^3)	Bouguecha et al. (2005)
SMADES project (experiment-scale)	Spiral-wound AGMD (with internal heat recovery function)	–	0.12 (120 L/day with)	Solar thermal-PV energy	±15 €/m^3	Banat et al. (2007a)
SMADES project	Solar powered MD (SP-MD)	Total = 98%	27 L/m^2 membrane surface area	Solar	18 €/m^3	Banat et al. (2007b)
Part of MEDESOL project	AGMD	–	240	Thermal (solar field)	1.85 €/m^3	Kullab (2011)
ISE Fraunhofer Institute	DCMD, AGMD, and VMD	–	–	Solar heater	DCMD = 12.7 USD/m^3, AGMD = 18.26 USD/m^3, VMD = 16.02 USD/m^3	Saffarini et al. (2012)
		–	–	Free heat	DCMD = 3.3 USD/m^3, AGMD = 5.4 USD/m^3, VMD = 2.2 USD/m^3	Saffarini et al. (2012)

that a looping single-stage gap MD operation cannot be economically competitive with RO unless they operate with brine concentrations greater than 75 g/L. For feed concentration in the range of 25–200 g/L and water recovery of 30–75%, the water cost ranges from USD 10–16/m^3. Though the water cost could be reduced by improving the intrinsic membrane properties, a substantial decrease in water cost would only be achieved by optimizing the heat recovery or utilizing cheaper heating and chilling sources and using cheaper heat exchangers (Bartholomew et al. 2020). These findings highlight the sensitivity of water production costs by MD on the thermal energy price. Due to higher water recovery at comparable energy requirements, a highly competitive water cost with respect to RO was indicated in an RO + MD configuration.

5 Zero liquid discharge (ZLD) seawater membrane distillation (SWMD)

While SWMD is hardly competitive with SWRO for straightforward desalination, SWMD's unique features open up possibilities for niche applications. The potential of SWMD to operate with extremely high salt-rejection highlights its potential for high-purity water production. A substantial amount of high-purity water is used in steam-electric power stations as the boiler feed (Bennett 2009; Kuipers et al. 2014). At present, high-purity water production from seawater is carried out through an established yet complex process incorporating several operation stages to reduce seawater TDS. The first stage is SWRO which operates with a water recovery of 45–50% (Ji et al. 2010; Choi et al. 2019a, b). Although a 99.5% salt rejection can be achieved by SWRO, the permeate of SWRO still has significant TDS ranged from 200 to 500 ppm (Bindels et al. 2020). Further purification is conducted in the brackish-water reverse-osmosis (BWRO) with permeate TDS ranging from 5-120 ppm, depending on seawater feed salinity (Bindels et al. 2020). Lastly, BWRO permeate is passed on to the ion exchange resin to further remove ions (Jacob 2007; Rahmawati et al. 2012; Wang et al. 2000). Intensification of the aforementioned process could be achieved by applying MD as a stand-alone unit operation (Figure 9a). In SWMD operation, the SWRO, BWRO and ion-exchange resin are eliminated and replaced by the MD unit. A high-pressure pump (HPP) and booster pump (BP) are also not required in this intensified process, which leads to a reduction in CAPEX. This further implies a reduction in OPEX, as the electrical work to generate the high pressure in SWRO contributes significantly to the energy requirement.

Another distinctive trait of SWMD is the ability to operate under ZLD conditions, in which high-purity water and valuable salts can be produced simultaneously. This paradigm puts an end to the economic and environmental impact that conventional brine management suffers from. This approach is in accordance with the more stringent environmental regulations and could transform the ZLD SWMD into energy and cost-intensive process. A solar-powered MD plant in the SMADES project has succeeded in recovering 98% of water during its operation. Further improvements could potentially result in absolute water-salt recovery. SWMD operating under ZLD conditions also focuses on highly valuable mineral recovery, such as magnesium, rubidium, phosphorus, nickel, cesium, and germanium (Dirach et al. 2005). In the bench-scale membrane distillation–crystallization (MDC) experiment carried out on RO brines, a NaCl crystal production of 17 kg/m^3 was produced with 90% water recovery (Ji et al. 2010). Quist–Jensen et al. (2016) operated an integrated-membrane system for simultaneous water and mineral recovery, which consisted of NF, RO, MD, and MCr (Figure 9b). The seawater was pretreated prior to NF to remove the hardness. NF permeate was further processed in RO, while the NF retentate was concentrated in a membrane crystallization (MCr) unit to produce water and salts. The RO retentate was treated in MD to increase the water recovery, then further concentrated in MCr. Salts of divalent ions, such as barium (in the form of $BaSO_4$), strontium (in the form of $SrSO_4$), and magnesium (in the form of $MgSO_4{\cdot}7H_2O$, epsomite) were recovered from the NF retentate via MCr. Meanwhile, lithium (in the form of LiCl) could only be recovered from the RO brine via MD and MCr. Recovery of KCl and NaCl was made from both NF and RO retentate. A pilot-scale simulation of this system indicated the recovery of 0.07 kg of $BaSO_4$ and 40 kg of $SrSO_4$ from 1 m^3 of NF retentate when MCr was operated at 80% water recovery. At water recovery of 86%, NaCl precipitated out from the NF retentate, followed by epsomite at a water recovery of 93%. LiCl could only be crystallized from the RO brine at a water recovery of 97%. In fact, the economic value of these salts might be higher than the water produced, hence could significantly offset the water cost. It is important to note that crystallization of valuable salts in SWMD occurs at a high water recovery of more than 80%; hence, efforts to achieve high water flux and delay flux decline are essential.

In general, there are three configurations for ZLD SWMD based on the location of the feed tank, crystallizer, and the membrane module. In the first configuration, the feed tank and crystallizer are two separate units. The feed solution is heated in the feed tank prior to being pumped to the

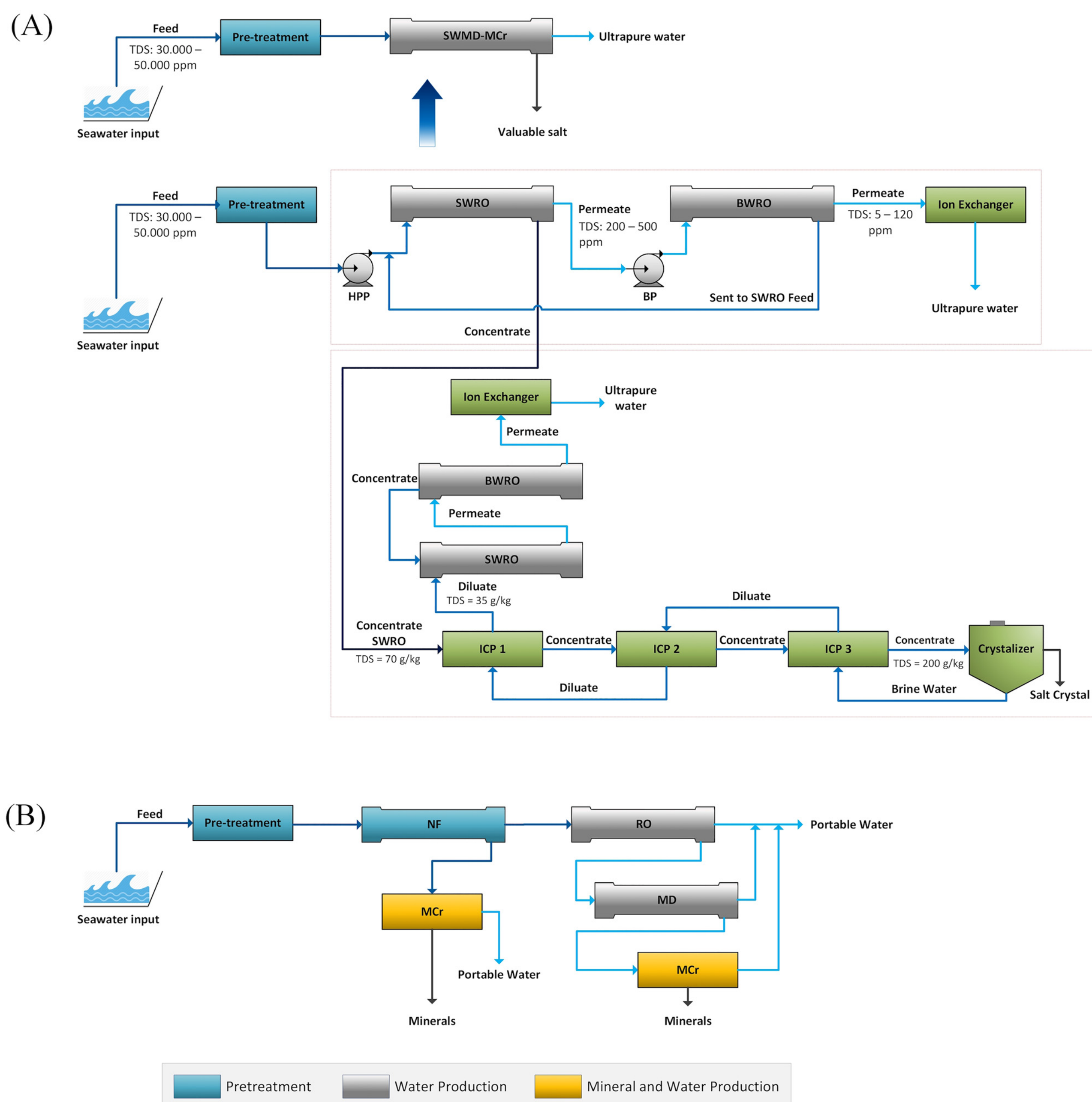

Figure 9: Schematic representation of (A) stand-alone SWMD compared to the hybrid ICP–SWRO for ZLD operation, and (B) an integrated RO–MD–MCr system with salt recovery (Quist-Jensen et al. 2016), published by MDPI.

membrane module where feed concentration takes place. The concentrated feed is then cooled in the crystallizer to promote salt precipitation. Afterward, the remaining solution is pumped back to the feed tank to be reheated and recirculated to the DCMD membrane module (Figure 10a). In this configuration, additional work is required to transfer the feed solution from the crystallizer back to the feed tank. The desire to eliminate this work leads to the second configuration in Figure 10b, where the feed tank is integrated with the crystallizer and operated in batch mode. In this configuration, the hot feed is circulated to the DCMD membrane module and pumped back to the feed tank at temperature of 60 °C. Once the feed solution reaches supersaturation, the circulation to the membrane module is stopped and the feed tank is acted as an evaporative crystallizer with a temperature of 70 °C to obtain crystals at the bottom of the feed tank/crystallizer. In the third configuration the feed tank is combined with the crystallizer; however, the membrane module

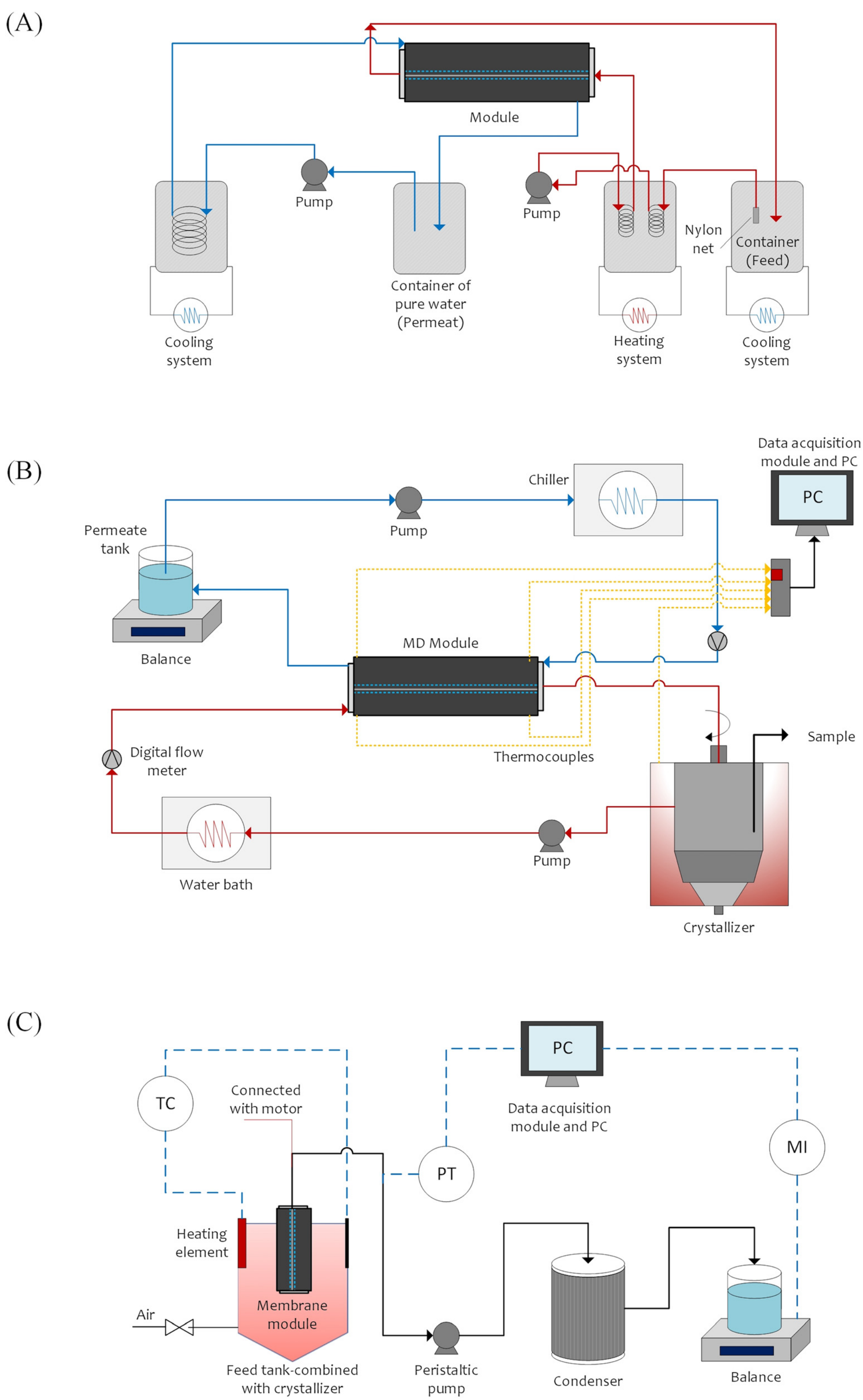

Figure 10: Schematic of a membrane-based ZLD system for SWMD with (A) separated feed tank and crystallizer (Wu et al. 1991), reproduced with permission from Elsevier; (B) the feed tank-combined crystallizer (Tun et al. 2005), reproduced with permission from Elsevier; and (C) submerged VMD in feed tank-combined crystallizer (Julian et al. 2016), reproduced with permission from Elsevier.

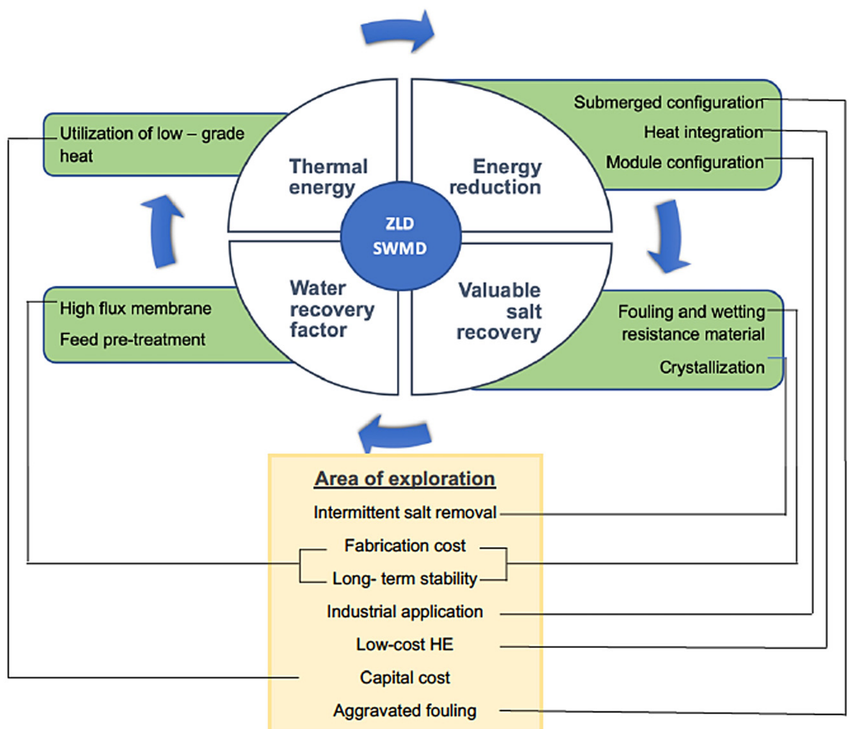

Figure 11: Summary of challenges, potential strategies, and future outlook for the scale-up of ZLD SWMD.

is immersed in the feed tank/crystallizer. The need for feed reheating and feed circulation are eliminated in the third configuration, and a more even temperature distribution along the membrane module can be achieved. The configuration of the system in Figure 10c is VMD, however, similar advantages apply for other MD submerged configuration (Meng et al. 2015) However, in contrast to the second configuration, fouling of negative temperature-solubility coefficient salts such as $CaCO_3$ impose disadvantages with this particular configuration (Julian et al. 2018).

Although more research is necessary, SWMD is still the most prominent technology for ZLD desalination to date. Another technology with a ZLD prospective is ion concentration polarization (ICP), which is a unipolar electro-membrane process that employs one type of ion exchange membrane. ICP has the capability to produce high-purity water and salt and is particularly attractive when combined with SWRO (Figure 9a). Cost evaluation of the ICP indicates that this process is viable when processing feed with a minimum concentration of 70 g/kg, which is approximately the concentration of the SWRO concentrate. With a maximum recovery of 50%, the dilute of the first ICP is set at a concentration of 35 g/kg and is fed to the SWRO for high-purity water production. The concentrate of the first ICP is further processed in a later stage of ICP to achieve a minimum concentration of 200 g/kg. The study recommends three-stages of IPC, which results in the lowest water cost. The salt concentration of the third ICP concentrate is suitable for crystallization. Though ZLD can be performed by ICP-SWRO technology, the cost is high, even when compared to the cost of SWMD. For the first ICP feed concentration of 70 g/kg, the water cost was $4/m^3 ICP dilute. To produce high-purity water, the water cost of SWRO ($0.5–$1.2/m^3) should be considered. For salt recovery under optimum conditions (three-stages of ICP), the total water cost of the three-stages of ICP was $21.7/m^3 and the crystallization cost was $40/ton of salt (Choi et al. 2019a, b).

6 Conclusions and future outlook

The perspective of the water-energy-environment nexus highlights the interstate connection of the security of water, energy, and environment. The concept of SWMD suggests MD capability to produce high-purity water with no restriction arises from osmotic pressure; hence, SWMD is able to gain higher recovery factor than that in SWRO. Accordingly, SWMD can be operated with a high concentration feed up to its supersaturation condition. Brine disposal is omitted in the ZLD operation by incorporating a crystallizer, so that the brine is separated into salt and high-purity water, producing two products with significant economic value. The summary of challenges, potential strategies, and the future outlook for the scale-up of ZLD SWMD is presented in Figure 11. The main setback of SWMD in general is energy consumption. The heating of the feed solution can be costly and the use of low-grade heat, such as waste heat, geothermal or solar energy, was emphasized in much of the research. Solar energy has been categorized as the most prominent low-cost energy for MD; however, solar collectors might substantially increase the capital cost of the plant, and further study on this subject is required.

Approaches for energy reduction, such as heat recovery and heat exchange, are among the most discussed topics in SWMD, especially as cooling has also been proven to be an energy-intensive step in SWMD. Also, reheating the feed to compensate for heat loss during circulation consumes a substantial amount of energy as well. A submerged SWMD configuration is one of the potential alternatives as feed circulation is eliminated. However, being a stand-alone SWMD, increased fouling propensity was a setback as fouling is aggravated at higher feed concentrations. The study of the submerged configuration is limited and mainly focused on scaling with a relatively low water recovery factor. More research on fouling removal strategies and more effort to pave the way towards a more robust submerged MD is necessary. To reduce the energy requirements, it is also essential to optimize the heat transfer, i.e. by reducing the temperature polarization and heat conduction through the membrane, which maximizes the thermal energy utilization. In regard to this, advancement in membrane modules and their configuration have yielded promising results, with reduced SEC and increased GOR due to the reduction of internal heat loss.

For the industrial application of SWMD, the cost of water production is the most vital parameter. To date, SWMD is restricted to pilot-scale applications, resulting in incredibly high water cost, and it should not be directly compared to a high-capacity SWRO plant. In general, the water cost decreases as the plant capacity increases, as indicated in a few modeling studies. However, the extent to which the water cost would be reduced by the increasing plant capacity is still questionable. Hence, in addition to the efforts on energy consumption reduction that accounts for 50–60 % of total water cost (Zarzo and Prats 2018), the water cost of SWRO could also be reduced by increasing the water recovery factor.

MD-specific membranes with tuned intrinsic properties possess outstanding flux as well as remarkable fouling and wetting resistance, hence provide a higher water recovery factor. However, extended study on the novel membrane stability and performance with actual seawater and extended operation time is required. The fabrication cost of the novel membranes on a large scale is also an area of interest, as it greatly affects the final water cost. Feed pretreatment, particularly to remove the hardness of the feed solution by using UF/NF also results in an excellent water recovery factor. At an increased water recovery factor, the supersaturation of salts in the feed stream can be obtained, enabling valuable-salt recovery at a specific water recovery factor. Even though each salt precipitates at a different water recovery factor, careful measures (such as periodic salt removal) should be taken to maintain the purity of the products, as cross-contamination of each specific salt may occur during crystallization. The high value of particular harvested salts, such as LiCl, $BaSO_4$, and $SRSO_4$, can offset the water cost of SWMD, and this opens up the possibility of economically-feasible ZLD SWMD. Despite all this, continued research – from laboratory to industrial-scale studies—is critical to push forward the application of ZLD SWMD.

Author contributions: All the authors have accepted responsibility for the entire content of this submitted manuscript and approved submission.

Research funding: The authors gratefully acknowledge the financial support from the Research Program provided by the Institut Teknologi Bandung (Riset ITB).

Conflict of interest statement: The authors declare that there is no conflict of interest regarding this article.

References

Abdel-Karim, A., Luque-Alled, J.M., Leaper, S., Alberto, M., Fan, X., Vijayaraghavan, A., Gad-Allah, T.A., El-Kalliny, A.S., Szekely, G., Ahmed, S.I.A., et al. (2019). PVDF membranes containing reduced graphene oxide: effect of degree of reduction on membrane distillation performance. Desalination 452: 196–207.

Abdelrasoul, A., Doan, H., and Lohi, A. (2017). Sustainable water technology and water-energy nexus. In: *Biomimetic and bioinspired membranes for new frontiers in sustainable water treatment technology*. IntechOpen, London, UK, pp. 1–12.

Abu-zeid, M.A.E., Zhang, L., Jin, W., Feng, T., Wu, Y., and Chen, H. (2016). Improving the performance of the air gap membrane distillation process by using a supplementary vacuum pump. Desalination 384: 31–42.

Adusei-Gyamfi, J., Ouddane, B., Rietveld, L., Cornard, J.P., and Criquet, J. (2019). Natural organic matter-cations complexation and its impact on water treatment: a critical review. Water Res. 160: 130–147.

Ahmad, A., Irfan, M., Lee, C., Park, C., and Kim, J. (2019). Hybrid organic-inorganic functionalized polyethersulfone membrane for hyper-saline feed with humic acid in direct contact membrane distillation. Separ. Purif. Technol. 210: 20–28.

Albeirutty, M., Turkmen, N., Al-sharif, S., Bouguecha, S., Malik, A., and Faruki, O. (2018). An experimental study for the characterization of fl uid dynamics and heat transport within the spacer- fi lled channels of membrane distillation modules. Desalination 430: 136–146.

Ali, A., Quist-Jensen, C.A., Macedonio, F., and Drioli, E. (2015). Application of membrane crystallization for minerals' recovery from produced water. Membranes 5: 772–792.

Ali, A., Tufa, R.A., Macedonio, F., Curcio, E., and Drioli, E. (2018). Membrane technology in renewable-energy-driven desalination. Renew. Sustain. Energy Rev. 81: 1–21.

Alkhudhiri, A., Darwish, N., and Hilal, N. (2012). Membrane distillation: a comprehensive review. Desalination 287: 2–18.

Alklaibi, A.M. and Lior, N. (2005). Membrane-distillation desalination: status and potential. Desalination 171: 111–131.

Alklaibi, A.M. and Lior, N. (2006). Heat and mass transfer resistance analysis of membrane distillation. J. Membr. Sci. 282: 362–369.

Alnouri, S.Y., Linke, P., and El-halwagi, M.M. (2018). Accounting for central and distributed zero liquid discharge options in interplant water network design. J. Clean. Prod. 171: 644–661.

Andrés-Mañas, J.A., Ruiz-Aguirre, A., Acién, F.G., and Zaragoza, G. (2018). Assessment of a pilot system for seawater desalination based on vacuum multi-effect membrane distillation with enhanced heat recovery. Desalination 443: 110–121.

Andrés-Mañas, J.A., Ruiz-Aguirre, A., Acién, F.G., and Zaragoza, G. (2020). Performance increase of membrane distillation pilot scale modules operating in vacuum-enhanced air-gap configuration. Desalination 475: 114202.

Angel, M., Bonnélye, V., and Cremer, G. (2006). Fujairah reverse osmosis plant: 2 years of operation. Desalination 3: 91–99.

Antony, A., How, J., Gray, S., Childress, A.E., Le-clech, P., and Leslie, G. (2011). Scale formation and control in high pressure membrane water treatment systems: a review. J. Membr. Sci. 383: 1–16.

Ashoor, B.B., Mansour, S., Giwa, A., Dufour, V., and Hasan, S.W. (2016). Principles and applications of direct contact membrane distillation (DCMD): a comprehensive review. Desalination 398: 222–246.

Asim, M., Uday Kumar, N.T., and Martin, A.R. (2016). Feasibility analysis of solar combi-system for simultaneous production of pure drinking water via membrane distillation and domestic hot water for single-family villa: pilot plant setup in Dubai. Desal. Water Treat. 57: 21674–21684.

Atkinson, S. (2020). *Memsift explores further markets for its technologies by focusing on North America*. New York: Elsevier.

Banat, F. and Jwaied, N. (2008). Economic evaluation of desalination by small-scale autonomous solar-powered membrane distillation units. Desalination 220: 566–573.

Banat, F., Jwaied, N., Rommel, M., and Koschikowski, J. (2007a). Desalination by a "compact SMADES" autonomous solar-powered membrane distillation unit. Desalination 217: 29–37.

Banat, F., Jwaied, N., Rommel, M., and Koschikowski, J. (2007b). Performance evaluation of the " large SMADES " autonomous desalination solar-driven membrane distillation plant in Aqaba, Jordan. Desalination 217: 17–28.

Bartholomew, T.V., Dudchenko, A.V., Siefert, N.S., and Mauter, S. (2020). Cost optimization of high recovery single stage gap membrane distillation. J. Membr. Sci. 611: 118370.

Bennett, A. (2009). High and ultra-high purity water. Filtrat. Separ. 46: 24–27.

Bernardes, P.C., de Andrade, N.J., da Silva, L.H.M., de Carvalho, A.F., Fernandes, P.É., Araújo, E.A., Lelis, C.A., Mol, P.C.G., and de Sá, J.P.N. (2014). Modification of polysulfone membrane used in the water filtration process to reduce biofouling. J. Nanosci. Nanotechnol. 14: 6355–6367.

Bindels, M., Carvalho, J., Bayona, C., Brand, N., and Nelemans, B. (2020). Techno-economic assessment of seawater reverse osmosis (SWRO) brine treatment with air gap membrane distillation (AGMD). Desalination 489: 114532.

Boo, C., Lee, J., and Elimelech, M. (2016). Omniphobic polyvinylidene fluoride (PVDF) membrane for desalination of shale gas produced water by membrane distillation. Environ. Sci. Technol. 50: 12275–12282.

Bouguecha, S., Hamrouni, B., and Dhahbi, M. (2005). Small scale desalination pilots powered by renewable energy sources: case studies. Desalination 183: 151–165.

Burgoyne, A. and Vahdati, M.M. (2005). Direct contact membrane distillation. Separ. Sci. Technol. 2005: 98–110.

Camacho, L.M., Dumée, L., Zhang, J., Li, J., Duke, M., Gomez, J., and Gray, S. (2013). Advances in membrane distillation for water desalination and purification applications. Water, https://doi.org/10.3390/w50x000x.

Cath, T.Y., Adams, V.D., and Childress, A.E. (2004). Experimental study of desalination using direct contact membrane distillation: a new approach to flux enhancement. J. Membr. Sci. 228: 5–16.

Chang, J., Zuo, J., Zhang, L., Brien, G.S.O., and Chung, T. (2017). Using green solvent, triethyl phosphate (TEP), to fabricate highly porous PVDF hollow fiber membranes for membrane distillation. J. Membr. Sci. 539: 295–304.

Chen, X., Gao, X., Fu, K., Qiu, M., Xiong, F., Ding, D., Cui, Z., Wang, Z., Fan, Y., and Drioli, E. (2018). Tubular hydrophobic ceramic membrane with asymmetric structure for water desalination via vacuum membrane distillation process. Desalination 443: 212–220.

Chen, T. and Ho, C. (2010). Immediate assisted solar direct contact membrane distillation in saline water desalination. J. Membr. Sci. 358: 122–130.

Chen, Y., Li, Y., and Chang, H. (2012). Optimal design and control of solar driven air gap membrane distillation desalination systems. Appl. Energy 100: 193–204.

Chen, Y., Lu, K.J., and Chung, T. (2020a). An omniphobic slippery membrane with simultaneous anti-wetting and anti-scaling properties for robust membrane distillation. J. Membr. Sci. 595: 117572.

Chen, Y., Lu, Y., Japip, S., and Chung, T. (2020b). Can composite Janus membranes with an ultrathin dense hydrophilic layer resist wetting in membrane distillation? Environ. Sci. Technol. 54: 12713–12722.

Chen, Y., Tian, M., Li, X., Wang, Y., An, A.K., Fang, J., and He, T. (2017). Anti-wetting behavior of negatively charged superhydrophobic PVDF membranes in direct contact membrane distillation of emulsified wastewaters. J. Membr. Sci. 535: 230–238.

Cheng, L., Zhao, Y., Li, P., Li, W., and Wang, F. (2018). Comparative study of air gap and permeate gap membrane distillation using internal heat recovery hollow fiber membrane module. Desalination 426: 42–49.

Chen, G., Yang, X., Lu, Y., Wang, R., and Fane, A.G. (2014). Heat transfer intensification and scaling mitigation in bubbling-enhanced membrane distillation for brine concentration. J. Membr. Sci. 470: 60–69.

Choi, S., Kim, B., Nayar, K.G., Yoon, J., Al-hammadi, S., V, J.H.L., Han, J., and Al-anzi, B. (2019a). Techno-economic analysis of ion concentration polarization desalination for high salinity desalination applications. Water Res. 155: 162–174.

Choi, Y., Naidu, G., Jeong, S., Lee, S., and Vigneswaran, S. (2018). Fractional-submerged membrane distillation crystallizer (F-SMDC) for treatment of high salinity solution. Desalination 440: 59–67.

Choi, Y., Ryu, S., Naidu, G., and Lee, S. (2019b). Integrated submerged membrane distillation-adsorption system for rubidium recovery. Separ. Purif. Technol. 218: 146–155.

Choo, K. and Stensel, H.D. (1998). Sequencing batch membrane reactor treatment: nitrogen removal and membrane fouling evaluation. Water Environ. Res. 72(4).

Christ, A., Regenauer-lieb, K., and Tong, H. (2014). Thermodynamic optimisation of multi effect distillation driven by sensible heat sources. Desalination 336: 160–167.

Chung, H.W., Swaminathan, J., Warsinger, D.M., and J.H.L., V. (2016). Multistage vacuum membrane distillation (MSVMD) systems for high salinity applications. J. Membr. Sci. 497: 128–141.

Chung, S., Seo, C.D., Lee, H., Choi, J., and Chung, J. (2014). Design strategy for networking membrane module and heat exchanger for direct contact membrane distillation process in seawater desalination. Desalination 349: 126–135.

Chunrui, W., Yue, J., Huayan, C., Xuan, W., Qijun, G., and Xiaolong, L. (2011). Study on air-bubbling strengthened membrane distillation process. Desal. Water Treat. 2011: 37–41.

Cipollina, A., Miceli, A. Di, Koschikowski, J., Micale, G., and Rizzuti, L. (2009). CFD simulation of a membrane distillation module channel. Desal. Water Treat. 2009: 177–183.

Criscuoli, A. (2016). Improvement of the membrane distillation performance through the integration of different configurations. Chem. Eng. Res. Des. 111: 316–322.

Curcio, E., Ji, X., Di, G., Obaidani, A., Fontananova, E., and Drioli, E. (2010). Membrane distillation operated at high seawater concentration factors: role of the membrane on $CaCO_3$ scaling in presence of humic acid. J. Membr. Sci. 346: 263–269.

Deng, L., Ngo, H.H., Guo, W., and Zhang, H. (2019). Pre-coagulation coupled with sponge-membrane filtration for organic matter removal and membrane fouling control during drinking water treatment. Water Res. 157: 155–166.

Dirach, J. Le, Nisan, S., and Poletiko, C. (2005). Extraction of strategic materials from the concentrated brine rejected by integrated nuclear desalination systems. Desalination 182: 449–460.

Dizge, N., Shaulsky, E., and Karanikola, V. (2019). Electrospun cellulose nanofibers for superhydrophobic and oleophobic membrane. J. Membr. Sci. 2019: 117271.

Dotremont, C., Kregersman, B., Sih, R., Lai, K.C., Koh, K., and Seah, H. (2010). Seawater desalination with memstill technology – a sustainable solution for the industry. Water Pract. Technol. 5: 1–7.

Drioli, E., Laganà, F., Criscuoli, A., and Barbieri, G. (1999). Integrated membrane operations in desalination processes. Desalination 122: 141–145.

Drioli, E., Curcio, E., Criscuoli, A., Di Profio, and Di, G. (2004). Integrated system for recovery of $CaCO_3$, NaCl and $MgSO_4{\cdot}7H_2O$ from nanofiltration retentate. J. Membr. Sci. 239: 27–38.

Drioli, E., Ali, A., and Macedonio, F. (2015). Membrane distillation: recent developments and perspectives. Desalination 356: 56–84.

Duong, H.C., Cooper, P., Nelemans, B., Cath, T.Y., and Nghiem, L.D. (2016). Evaluating energy consumption of air gap membrane distillation for seawater desalination at pilot scale level. Separ. Purif. Technol. 166: 55–62.

El-Bourawi, M.S., Ding, Z., Ma, R., and Khayet, M. (2006). A framework for better understanding membrane distillation separation process. J. Membr. Sci. 285: 4–29.

Eltawil, M.A., Zhengming, Z., and Yuan, L. (2009). A review of renewable energy technologies integrated with desalination systems. Renew. Sustain. Energy Rev. 13: 2245–2262.

Fan, H. and Peng, Y. (2012). Application of PVDF membranes in desalination and comparison of the VMD and DCMD processes. Chem. Eng. Sci. 79: 94–102.

Flemming, H.C. (1997). Reverse osmosis membrane biofouling. Exp. Therm. Fluid Sci. 14: 382–391.

Francis, L., Ghaffour, N., Alsaadi, A.A., and Amy, G.L. (2013). Material gap membrane distillation : a new design for water vapor flux enhancement. J. Membr. Sci. 448: 240–247.

Fritzmann, C., Löwenberg, J., Wintgens, T., and Melin, T. (2007). State-of-the-art of reverse osmosis desalination. Desalination 216: 1–76.

Gil, J.D., Roca, L., Ruiz-Aguirre, A., Zaragoza, G., and Berenguel, M. (2018a). Optimal operation of a solar membrane distillation pilot plant via nonlinear model predictive control. Comput. Chem. Eng. 109: 151–165.

Gil, J.D., Roca, L., Zaragoza, G., and Berenguel, M. (2018b). A feedback control system with reference governor for a solar membrane distillation pilot facility. Renew. Energy 120: 536–549.

Glueckstern, P., Priel, M., and Wilf, M. (2002). Field evaluation of capillary UF technology as a pretreatment for large seawater RO systems. Desalination 147: 55–62.

González, D., Amigo, J., and Suárez, F. (2017). Membrane distillation: perspectives for sustainable and improved desalination. Renew. Sustain. Energy Rev. 80: 238–259.

Gopi, G., Arthanareeswaran, G., and Ismail, A.F. (2019). Perspective of renewable desalination by using membrane distillation. Chem. Eng. Res. Des. 144: 520–537.

Gordon, J.M. and Hui, T.C. (2016). Thermodynamic perspective for the specific energy consumption of seawater desalination. Desalination 386: 13–18.

Gryta, M. (2005). Long-term performance of membrane distillation process. J. Membr. Sci. 265: 153–159.

Gryta, M. (2008a). Alkaline scaling in the membrane distillation process. Desalination 228: 128–134.

Gryta, M. (2008b). Fouling in direct contact membrane distillation process. J. Membr. Sci. 325: 383–394.

Gryta, M. (2009). Calcium sulphate scaling in membrane distillation process. Chem. Pap. 63: 146–151.

Guan, G., Yang, X., Wang, R., and Fane, A.G. (2015). Evaluation of heat utilization in membrane distillation desalination system integrated with heat recovery. Desalination 366: 80–93.

Guillén-Burrieza, E., Alarcón-padilla, D., Palenzuela, P., and Zaragoza, G. (2015). Techno-economic assessment of a pilot-scale plant for solar desalination based on existing plate and frame MD technology. Desalination 374: 70–80.

Guillén-Burrieza, E., Blanco, J., Zaragoza, G., Alarcón, D.C., Palenzuela, P., Ibarra, M., and Gernjak, W. (2011). Experimental analysis of an air gap membrane distillation solar desalination pilot system. J. Membr. Sci. 379: 386–396.

Hagedorn, A., Fieg, G., Winter, D., Koschikowski, J., Grabowski, A., and Mann, T. (2017). Membrane and spacer evaluation with respect to future module design in membrane distillation. Desalination 413: 154–167.

He, F., Sirkar, K.K., and Gilron, J. (2009). Studies on scaling of membranes in desalination by direct contact membrane distillation : $CaCO_3$ and mixed $CaCO_3/CaSO_4$ systems. Chem. Eng. Sci. 64: 1844–1859.

Hettiarachchi, T.R. (2015). *Applications study of membrane distillation for the dairy industry*, Master of Science thesis. Melbourne: Institute for Sustainability and Innovation, Victoria University.

Hickenbottom, K.L. and Cath, T.Y. (2014). Sustainable operation of membrane distillation for enhancement of mineral recovery from hypersaline solutions. J. Membr. Sci. 454: 426–435.

Huang, Y.X., Wang, Z., Hou, D., and Lin, S. (2017a). Coaxially electrospun super-amphiphobic silica-based membrane for anti-surfactant-wetting membrane distillation. J. Membr. Sci. 531: 122–128.

Huang, Y.X., Wang, Z., Jian Jin, A., and Lin, S. (2017b). A novel Janus membrane for membrane distillation with simultaneous fouling and wetting resistance. Environ. Sci. Technol. 51: 13304–13310.

Hubadillah, S.K., Othman, M.H.D., Matsuura, T., Rahman, M.A., Jaafar, J., Ismail, A.F., and Amin, S.Z.M. (2018). Green silica-based ceramic hollow fiber membrane for seawater desalination via direct contact membrane distillation. Separ. Purif. Technol. 205: 22–31.

Hubadillah, S.K., Othman, M.H.D., Ismail, A.F., Rahman, M.A., and Jaafar, J. (2019). A low cost hydrophobic kaolin hollow fiber membrane (h-KHFM) for arsenic removal from aqueous solution via direct contact membrane distillation. Separ. Purif. Technol. 214: 31–39.

Im, B.G., Lee, J.G., Kim, Y.D., and Kim, W.S. (2018). Theoretical modeling and simulation of AGMD and LGMD desalination processes using a composite membrane. J. Membr. Sci. 565: 14–24.

Ismail, F., Khulbe, K.C., and Matsuura, T. (2018). *Reverse osmosis*. New York: Elsevier.

Izquierdo-Gil, M.A., and Jonsson, G. (2003). Factors affecting flux and ethanol separation performance in vacuum membrane distillation (VMD). J. Membr. Sci. 214: 113–130.

Jaafar, S. and Sarbatly, R. (2015). Geothermal water desalination by using nanofiber membrane. *International Conference on Chemical, Environmental and Biological Sciences (ICCEBS'2012) Penang, Malaysia*.

Jabed, M., Bappy, P., Bahar, R., and Ariff, T.F. (2016). Effect of air gap in the performance of AGMD system. J. Eng. Appl. Sci. 11: 4087–4093.

Jacob, C. (2007). Seawater desalination: boron removal by ion exchange technology. Desalination 205: 47–52.

Jansen, A.E., Assink, J.W., Hanemaaijer, J.H., Medevoort, J. Van, and Sonsbeek, E. Van. (2013). Development and pilot testing of full-scale membrane distillation modules for deployment of waste heat. Desalination 323: 55–65.

Ji, X., Curcio, E., Al, S., Di, G., Fontananova, E., and Drioli, E. (2010). Membrane distillation-crystallization of seawater reverse osmosis brines. Separ. Purif. Technol. 71: 76–82.

Jiang, L., Chen, L., and Zhu, L. (2020). Fouling process of membrane distillation for seawater desalination : an especial focus on the thermal-effect and concentrating-effect during biofouling. Desalination 485: 114457.

Jiang, X., Tuo, L., Lu, D., Hou, B., Chen, W., and He, G. (2017). Progress in membrane distillation crystallization: process models, crystallization control and innovative applications. Front. Chem. Sci. Eng. 11: 647–662.

Joo, H.J. and Kwak, H.Y. (2016). Freshwater production characteristics of vacuum membrane distillation module for seawater desalination using a solar thermal system by seawater feed conditions. Desal. Water Treat. 57: 24645–24653.

Julian, H. (2018). *Process optimization and study of fouling in submerged vacuum membrane distillation and crystallization*, PhD thesis. Sydney: School of Chemical Engineering, UNSW.

Julian, H., Meng, S., Li, H., Ye, Y., and Chen, V. (2016). Effect of operation parameters on the mass transfer and fouling in submerged vacuum membrane distillation crystallization (VMDC) for inland brine water treatment. J. Membr. Sci. 520: 679–692.

Julian, H., Ye, Y., Li, H., and Chen, V. (2018). Scaling mitigation in submerged vacuum membrane distillation and crystallization (VMDC) with periodic air-backwash. J. Membr. Sci. 547: 19–33.

Karakulski, K., Gryta, M., and Morawski, A. (2002). Membrane processes used for potable water quality improvement. Desalination 145: 1–5.

Karakulski, K., Gryta, M., and Sasim, M. (2006). Production of process water using integrated membrane processes. In: *33rd International Conference of the Slovak Society of Chemical Engineering, 22—26 May 2006*. Tatranské Matliare.

Karbasi, E., Karimi-Sabet, J., Mohammadi-Rovshandeh, J., Ali Moosavian, M., Ahadi, H., and Amini, Y. (2017). Experimental and numerical study of air-gap membrane distillation (AGMD): novel AGMD module for Oxygen-18 stable isotope enrichment. Chem. Eng. J. 322: 667–678.

Kayvani, A., Rhad, T., Khraisheh, M., Atieh, M.A., Khraisheh, M., and Hilal, N. (2016). Reducing flux decline and fouling of direct contact membrane distillation by utilizing thermal brine from MSF desalination plant. Desalination 379: 172–181.

Khadijah, S., Ha, M., Othman, D., and Matsuura, T. (2018). Green silica-based ceramic hollow fiber membrane for seawater desalination via direct contact membrane distillation. Separ. Purif. Technol. 205: 22–31.

Khalifa, A.E. and Alawad, S.M. (2018). Air gap and water gap multistage membrane distillation for water desalination. Desalination 437: 175–183.

Khalifa, A.E., Alawad, S.M., and Antar, M.A. (2017). Parallel and series multistage air gap membrane distillation. Desalination 417: 69–76.

Khan, A.A., Siyal, M.I., Lee, C.K., Park, C., and Kim, J.O. (2019). Hybrid organic-inorganic functionalized polyethersulfone membrane for hyper-saline feed with humic acid in direct contact membrane distillation. Separ. Purif. Technol. 210: 20–28.

Khayet, M. (2011). Membranes and theoretical modeling of membrane distillation: a review. Adv. Colloid Interface Sci. 164: 56–88.

Khayet, M., Mengual, J.I., and Matsuura, T. (2005). Porous hydrophobic/hydrophilic composite membranes Application in desalination using direct contact membrane distillation. J. Membr. Sci. 252: 101–113.

Khayet, M., García-Payo, C., and Matsuura, T. (2019). Superhydrophobic nanofibers electrospun by surface segregating fluorinated amphiphilic additive for membrane distillation. J. Membr. Sci. 588: 117215.

Kiefer, F., Spinnler, M., and Sattelmayer, T. (2018). Multi-effect vacuum membrane distillation systems: model derivation and calibration. Desalination 438: 97–111.

Kim, J. and Hong, S. (2018). A novel single-pass reverse osmosis con fi guration for high-purity water production and low energy consumption in seawater desalination. Desalination 429: 142–154.

Kola, A., Ye, Y., Ho, A., Le-clech, P., and Chen, V. (2012). Application of low frequency transverse vibration on fouling limitation in

submerged hollow fibre membranes. J. Membr. Sci.: 54–65, 409–410, https://doi.org/10.1016/j.memsci.2012.03.017.
Koschikowski, J., Wieghaus, M., and Rommel, M. (2003). Solar thermal-driven desalination plants based on membrane distillation. Desalination 156: 295–304.
Koschikowski, J.Ã., Wieghaus, M., Rommel, M., Subiela, V., Rosa, J., Rodrı, B., and Pen, B. (2009). Experimental investigations on solar driven stand-alone membrane distillation systems for remote areas. Desalination 248: 125–131.
Kuipers, N., Leerdam, R. Van, Medevoort, J. Van, Tongeren, W. Van, Verelst, L., Vermeersch, M., and Corbisier, D. (2014). Techno-economic assessment of boiler feed water production by membrane distillation with reuse of thermal waste energy from cooling water. Desal. Treat 2014: 37–41.
Kujawa, J. (2019). From nanoscale modification to separation - the role of substrate and modifiers in the transport properties of ceramic membranes in membrane distillation. J. Membr. Sci. 580: 296–306.
Kullab, A. (2011). *Desalination using membrane distillation experimental and numerical study*, Doctoral Thesis. Stockholm: Royal Institute of Technology.
Laganà, F., Barbieri, G., and Drioli, E. (2000). Direct contact membrane distillation: modelling and concentration experiments. J. Membr. Sci. 166: 1–11.
Lawson, K.W. and Lloyd, D.R. (1996). Membrane distillation. II. Direct contact MD. J. Membr. Sci. 120: 123–133.
Lawson, K.W. and Lloyd, D.R. (1997). Membrane distillation. J. Membr. Sci. 124: 1–25.
Leaper, S., Abdel-Karim, A., Faki, B., Luque-Alled, J.M., Alberto, M., Vijayaraghavan, A., Holmes, S.M., Szekely, G., Badawy, M.I., Shokri, N., et al. (2018). Flux-enhanced PVDF mixed matrix membranes incorporating APTS-functionalized graphene oxide for membrane distillation. J. Membr. Sci. 554: 309–323.
Lee, J., Kim, W., Choi, J., Ghaffour, N., and Kim, Y. (2016). A novel multi-stage direct contact membrane distillation module: design, experimental and theoretical approaches. Water Res. 107: 47–56.
Li, C., Goswami, Y., and Stefanakos, E. (2013). Solar assisted sea water desalination: a review. Renew. Sustain. Energy Rev. 19: 136–163.
Li, X., Zhang, Y., Cao, J., Wang, X., Cui, Z., Zhou, S., Li, M., Drioli, E., Wang, Z., and Zhao, S. (2019). Enhanced fouling and wetting resistance of composite Hyflon AD/poly (vinylidene fluoride) membrane in vacuum membrane distillation. Separ. Purif. Technol. 211: 135–140.
Liu, R., Qin, Y., Li, X., and Liu, L. (2012). Concentrating aqueous hydrochloric acid by multiple-effect membrane distillation. Front. Chem. Sci. Eng. 6: 311–321.
Lorain, O., Hersant, B., Persin, F., Grasmick, A., Brunard, N., and Espenan, J.M. (2007). Ultrafiltration membrane pre-treatment benefits for reverse osmosis process in seawater desalting. Quantification in terms of capital investment cost and operating cost reduction. Desalination 203: 277–285.
Lu, K.J., Zuo, J., Chang, J., Kuan, H.N., and Chung, T.-S. (2018). Omniphobic hollow fiber membranes for vacuum membrane distillation. Environ. Sci. Technol. 52: 4472–4480.
Lu, K.J., Zuo, J., and Chung, T.S. (2017). Novel PVDF membranes comprising n-butylamine functionalized graphene oxide for direct contact membrane distillation. J. Membr. Sci. 539: 34–42.
Lu, K.J., Chen, Y., and Chung, T. (2019a). Design of omniphobic interfaces for membrane distillation: a review. Water Res. 162: 64–77.
Lu, K.J., Cheng, Z.L., Chang, J., Luo, L., and Chung, T. (2019b). Design of zero liquid discharge desalination (ZLDD) systems consisting of freeze desalination, membrane distillation, and crystallization powered by green energies. Desalination 458: 66–75.
Lu, X., Peng, Y., Ge, L., Lin, R., Zhu, Z., and Liu, S. (2016). Amphiphobic PVDF composite membranes for anti-fouling direct contact membrane distillation. J. Membr. Sci. 505: 61–69.
Luo, L., Zhao, J., and Chung, T.S. (2018). Integration of membrane distillation (MD) and solid hollow fiber cooling crystallization (SHFCC) systems for simultaneous production of water and salt crystals. J. Membr. Sci. 564: 905–915.
Ma, H., Hakim, L.F., Bowman, C.N., and Davis, R.H. (2001). Factors affecting membrane fouling reduction by surface modification and backpulsing. J. Membr. Sci. 189: 255–270.
Ma, Q., Ahmadi, A., and Cabassud, C. (2018). Direct integration of a vacuum membrane distillation module within a solar collector for small-scale units adapted to seawater desalination in remote places: design, modeling & evaluation of a fl at-plate equipment. J. Membr. Sci. 564: 617–633.
Macedonio, F., and Drioli, E. (2019). Membrane distillation development. Sustain. Water Wastewater Process 133–159, https://doi.org/10.1016/B978-0-12-816170-8.00005-3.
Maddah, H. and Chogle, A. (2017). Biofouling in reverse osmosis: phenomena, monitoring, controlling and remediation. Appl. Water Sci. 7: 2637–2651.
Martinez-Diez, L. and Vazquez-Gonzalez, M.I. (1998). Study of membrane distillation using channel spacers. J. Membr. Sci. 144: 45–56.
Martínez, L. and Rodríguez-Maroto, J.M. (2006). Characterization of membrane distillation modules and analysis of mass flux enhancement by channel spacers. J. Membr. Sci. 274: 123–137.
Martínez, L. and Rodríguez-Maroto, J.M. (2007). Effects of membrane and module design improvements on flux in direct contact membrane distillation. Desalination 205: 97–103.
Meindersma, G.W., Guijt, C.M., and Haan, A.B. De. (2006). Desalination and water recycling by air gap membrane distillation. Desalination 187: 291–301.
Meng, F., Chae, S.R., Drews, A., Kraume, M., Shin, H.S., and Yang, F. (2009). Recent advances in membrane bioreactors (MBRs): membrane fouling and membrane material. Water Res. 43: 1489–1512.
Meng, S., Hsu, Y., Ye, Y., and Chen, V. (2015). Submerged membrane distillation for inland desalination applications. Desalination 361: 72–80.
Mericq, J.P., Laborie, S., and Cabassud, C. (2010). Vacuum membrane distillation of seawater reverse osmosis brines. Water Res. 44: 5260–5273.
Mericq, J., Laborie, S., and Cabassud, C. (2011). Evaluation of systems coupling vacuum membrane distillation and solar energy for seawater desalination. Chem. Eng. J. 166: 596–606.
Mohamed, E.S., Boutikos, P., Mathioulakis, E., and Belessiotis, V. (2017). Experimental evaluation of the performance and energy efficiency of a vacuum multi-effect membrane distillation system. Desalination 408: 70–80.
Naidu, G., Geun, W., Jeong, S., Choi, Y., Ghaffour, N., and Vigneswaran, S. (2017). Transport phenomena and fouling in vacuum enhanced direct contact membrane distillation:

experimental and modelling. Separ. Purif. Technol. 172: 285–295.
Nghiem, L.D. and Cath, T. (2011). A scaling mitigation approach during direct contact membrane distillation. Separ. Purif. Technol. 80: 315–322.
Pantoja, C.E., Nariyoshi, Y.N., and Seckler, M.M. (2016). Membrane distillation crystallization applied to brine desalination: additional design criteria. Ind. Eng. Chem. Res. 55: 1004–1012.
Patil, D.K. and Shirsat, S.P. (2017). Membrane distillation review and flux prediction in direct contact membrane distillation process. Int Res J Eng Technol (IRJET) 2017: 829–845.
Phattaranawik, J., Jiraratananon, R., Fane, A.G., and Halim, C. (2001). Mass flux enhancement using spacer filled channels in direct contact membrane distillation. J. Membr. Sci. 187: 193–201.
Phattaranawik, J., Jiraratananon, R., and Fane, A.G. (2003). Heat transport and membrane distillation coefficients in direct contact membrane distillation. J. Membr. Sci. 212: 177–193.
Plattner, J., Naidu, G., Wintgens, T., Vigneswaran, S., and Kazner, C. (2017). Fluoride removal from groundwater using direct contact membrane distillation (DCMD) and vacuum enhanced DCMD (VEDCMD). Separ. Purif. Technol. 180: 125–132.
Quist-Jensen, C., Macedonio, F., and Drioli, E. (2016). Integrated membrane desalination systems with membrane crystallization units for resource recovery: a new approach for mining from the sea. Crystals 6: 36.
Ragunath, S., Roy, S., and Mitra, S. (2018). Carbon nanotube immobilized membrane with controlled nanotube incorporation via phase inversion polymerization for membrane distillation based desalination. Separ. Purif. Technol. 194: 249–255.
Rahmawati, K., Ghaffour, N., Aubry, C., and Amy, G.L. (2012). Boron removal efficiency from Red Sea water using different SWRO/ BWRO membranes. J. Membr. Sci. 423–424: 522–529.
Rattananurak, W., Chang, J., Wattanachira, S., Johir, M.A.H., and Vigneswaran, S. (2014). A novel plate settler in immersed membrane bioreactor (iMBR) in reducing membrane fouling. Desal. Water Treat 2014: 37–41.
Ray, S.S., Chen, S., Chang, H., and Dan, N. (2018). Enhanced desalination using a three-layer OTMS based superhydrophobic membrane for a membrane distillation process. RSC Adv. 8: 9640–9650.
Razmjou, A., Arifin, E., Dong, G., Mansouri, J., and Chen, V. (2012). Superhydrophobic modification of TiO 2 nanocomposite PVDF membranes for applications in membrane distillation. J. Membr. Sci. 415–416: 850–863.
Rezaei, M., Warsinger, D.M., Duke, M.C., Matsuura, T., and Samhaber, W.M. (2018). Wetting phenomena in membrane distillation: mechanisms, reversal, and prevention. Water Res. 139: 329–352.
Ruiz-Aguirre, A., Andrés-Mañas, J.A., Fernandez-Sevilla, J.M., and Zaragoza, G. (2017). Comparative characterization of three commercial spiral-wound membrane distillation modules. Desal. Water Treat. 61: 152–159.
Ruiz-Aguirre, A., Andrés-Mañas, J.A., Fernández-Sevilla, J.M., and Zaragoza, G. (2018). Experimental characterization and optimization of multi-channel spiral wound air gap membrane distillation modules for seawater desalination. Separ. Purif. Technol. 205: 212–222.
Saffarini, R.B., Summers, E.K., Arafat, H.A., and V, J.H.L. (2012). Economic evaluation of stand-alone solar powered membrane distillation systems. Desalination 299: 55–62.
Salmón, I.R. and Luis, P. (2018). Membrane crystallization via membrane distillation. Chem. Eng. Process 123: 258–271.
Sarbatly, R., and Chiam, C. (2013). Evaluation of geothermal energy in desalination by vacuum membrane distillation. Appl. Energy 112: 737–746.
Sauvet-Goichon, B. (2007). Ashkelon desalination plant - a successful challenge. Desalination 203: 75–81.
Scaffold, E.N., Lee, J., Boo, C., Ryu, W., Taylor, A.D., and Elimelech, M. (2016). Development of omniphobic desalination membranes using a charged development of omniphobic desalination membranes using a charged electrospun nanofiber scaffold. Appl. Mater. Interfaces 2016: 2–10.
Schofield, R.W., Fane, A.G., and Fell, C.J.D. (1987). Heat and mass transfer in membrane distillation. J. Membr. Sci. 33: 299–313.
Schwantes, R., Bauer, L., Chavan, K., Dücker, D., Felsmann, C., and Pfafferott, J. (2018). Air gap membrane distillation for hypersaline brine concentration: operational analysis of a full-scale module–New strategies for wetting mitigation. Desalination 444: 13–25.
Seo, D.H., Woo, Y.C., Xie, M., Murdock, A.T., Ang, E.Y.M., Jiao, Y., Park, M.J., Lim, S. Il, Lawn, M., et al. (2018). Anti-fouling graphene-based membranes for effective water desalination. Nat. Commun. 2018: 1–12.
Shahu, V.T. and Thombre, S.B. (2019). Air gap membrane distillation: a review. J. Renew. Sustain. Energy, https://doi.org/10.1063/1.5063766.
Shahzad, M.W. (2019). A standard primary energy approach for comparing desalination processes. NPJ Clean Water 2019: 1–7.
Shan, H., Liu, J., Li, X., Li, Y., and Tezel, F.H. (2018). Nanocoated amphiphobic membrane for flux enhancement and comprehensive anti-fouling performance in direct contact membrane distillation. J. Membr. Sci. 567: 166–180.
Shimokawa, A. (2009). Desalination plant with unique methods in Fukuoka. In: *Governmental Conference on Drinking Water Quality Management and Wastewater Control*. FUKUOKA District Waterworks Agency, Japan, pp. 1–14.
Stavrakakis, C., Sauvade, P., Coelho, F., and Moulin, P. (2018). Air backwash efficiency on organic fouling of UF membranes applied to shellfish hatchery effluents. Membranes, https://doi.org/10.3390/membranes8030048.
Summers, E.K., Arafat, H.A., and V, J.H.L. (2012). Energy efficiency comparison of single-stage membrane distillation (MD) desalination cycles in different configurations. Desalination 290: 54–66.
Swaminathan, J., Won, H., Warsinger, D.M., Almarzooqi, F.A., Arafat, H.A., and V, J.H.L. (2016). Energy efficiency of permeate gap and novel conductive gap membrane distillation. J. Membr. Sci. 502: 171–178.
Thomas, N., Mavukkandy, M.O., Loutatidou, S., and Arafat, H.A. (2017). Membrane distillation research & implementation: lessons from the past five decades. Separ. Purif. Technol. 189: 108–127.
Tijing, L.D., Chul, Y., Choi, J., Lee, S., Kim, S., and Kyong, H. (2015). Fouling and its control in membrane distillation - a review. J. Membr. Sci. 475: 215–244.
Tijing, L.D., Woo, Y.C., Shim, W.G., He, T., Choi, J.S., Kim, S.H., and Shon, H.K. (2016). Superhydrophobic nanofiber membrane containing carbon nanotubes for high-performance direct contact membrane distillation. J. Membr. Sci. 502: 158–170.

Tun, C.M., Fane, A.G., Matheickal, J.T., and Sheikholeslami, R. (2005). Membrane distillation crystallization of concentrated salts - flux and crystal formation. J. Membr. Sci. 257: 144–155.

Ullah, I. and Rasul, M.G. (2019). Recent developments in solar thermal desalination technologies: a review. Energies 12.

Wang, J., Wang, S., and Jin, M. (2000). A study of the electrodeionization process high-purity water production with a RO/EDI system. Desalination 132: 349–352.

Wang, P. and Chung, T. (2015). Recent advances in membrane distillation processes: membrane development, configuration design and application exploring. J. Membr. Sci. 474: 39–56.

Warsinger, D.M., Swaminathan, J., Guillen-Burrieza, E., Arafat, H.A., and V, J.H.L. (2015). Scaling and fouling in membrane distillation for desalination applications: a review. Desalination 356: 294–313.

Winter, D., Koschikowski, J., and Ripperger, S. (2012). Desalination using membrane distillation : flux enhancement by feed water deaeration on spiral-wound modules. J. Membr. Sci. 423–424: 215–224.

Wu, Y., Kong, Y., Liu, J., Zhang, J., and Xu, J. (1991). An experimental study on membrane distillation-crystallization for treating waste water in taurine production. Desalination 80: 235–242.

Xu, K., Feng, B., Zhou, C., and Huang, A. (2016). Synthesis of highly stable graphene oxide membranes on polydopamine functionalized supports for seawater desalination. Chem. Eng. Sci. 146: 159–165.

Xu, Z., Liu, Z., Song, P., and Xiao, C. (2017). Fabrication of super-hydrophobic polypropylene hollow fiber membrane and its application in membrane distillation. Desalination 414: 10–17.

Yan, K.K., Jiao, L., Lin, S., Ji, X., Lu, Y., and Zhang, L. (2018). Superhydrophobic electrospun nanofiber membrane coated by carbon nanotubes network for membrane distillation. Desalination 437: 26–33.

Yao, M., Tijing, L.D., Naidu, G., Kim, S., Matsuyama, H., Fane, A.G., and Kyong, H. (2020). A review of membrane wettability for the treatment of saline water deploying membrane distillation. Desalination 479: 114312.

Zaragoza, G. (2018). Commercial scale membrane distillation for solar desalination. npj Clean Water 2018: 1–6.

Zaragoza, G., Ruiz-Aguirre, A., and Guillén-Burrieza, E. (2014). Efficiency in the use of solar thermal energy of small membrane desalination systems for decentralized water production. Appl. Energy 130: 491–499.

Zarzo, D. and Prats, D. (2018). Desalination and energy consumption. What can we expect in the near future? Desalination 427: 1–9.

Zhang, J.W., Fang, H., Wang, J.W., Hao, L.Y., Xu, X., and Chen, C.S. (2014). Preparation and characterization of silicon nitride hollow fiber membranes for seawater desalination. J. Membr. Sci. 450: 197–206.

Zhang, Y., Peng, Y., Ji, S., Li, Z., and Chen, P. (2015). Review of thermal efficiency and heat recycling in membrane distillation processes. Desalination 367: 223–239.

Zhang, Y., Peng, Y., Ji, S., Qi, J., and Wang, S. (2017). Numerical modeling and economic evaluation of two multi-e ff ect vacuum membrane distillation (ME-VMD) processes. Desalination 419: 39–48.

Zhao, K., Heinzl, W., Wenzel, M., Büttner, S., Bollen, F., Lange, G., Heinzl, S., and Sarda, N. (2013). Experimental study of the memsys vacuum-multi-effect-membrane-distillation (V-MEMDf) module. Desalination 323: 150–160.

Zodrow, K.R., Bar-Zeev, E., Giannetto, M.J., and Elimelech, M. (2014). Biofouling and microbial communities in membrane distillation and reverse osmosis. Environ. Sci. Technol. 48: 13155–13164.

Zou, T., Dong, X., Kang, G., Zhou, M., Li, M., and Cao, Y. (2018). Fouling behavior and scaling mitigation strategy of $CaSO_4$ in submerged vacuum membrane distillation. Desalination 425: 86–93.

1. Copy dari website jurnal terkait issue jurnal yang memuat paper penulis

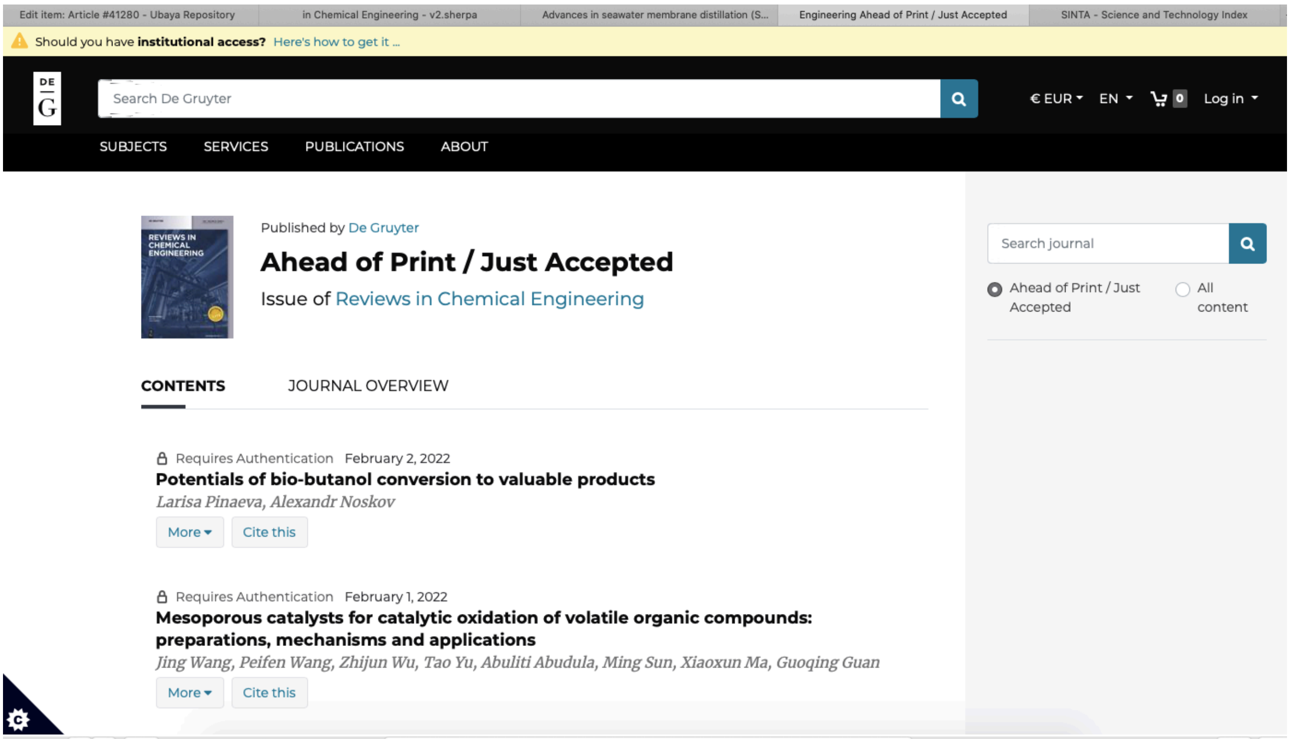

Edit item: Article #41280 - Ubaya Repository | in Chemical Engineering - v2.sherpa | Advances in seawater membrane distillation (S... | Engineering Ahead of Print / Just Accepted | SINTA - Science and Technology Index

Should you have **institutional access?** Here's how to get it ...

Search De Gruyter

€ EUR EN 0 Log in

SUBJECTS SERVICES PUBLICATIONS ABOUT

Published by De Gruyter

Ahead of Print / Just Accepted

Issue of Reviews in Chemical Engineering

Search journal

Ahead of Print / Just Accepted   All content

CONTENTS   JOURNAL OVERVIEW

Requires Authentication February 2, 2022
Potentials of bio-butanol conversion to valuable products
Larisa Pinaeva, Alexandr Noskov
More Cite this

Requires Authentication February 1, 2022
Mesoporous catalysts for catalytic oxidation of volatile organic compounds: preparations, mechanisms and applications
Jing Wang, Peifen Wang, Zhijun Wu, Tao Yu, Abuliti Abudula, Ming Sun, Xiaoxun Ma, Guoqing Guan
More Cite this

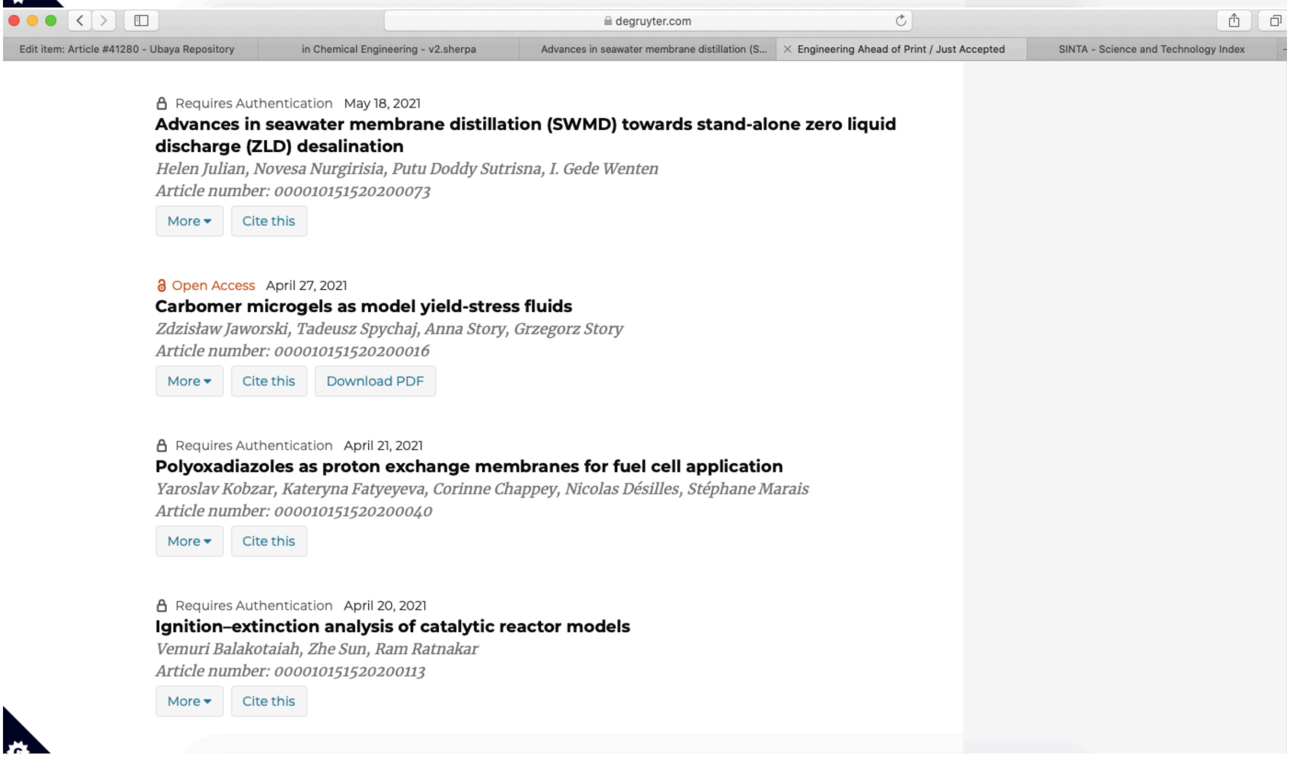

degruyter.com

Edit item: Article #41280 - Ubaya Repository | in Chemical Engineering - v2.sherpa | Advances in seawater membrane distillation (S... | Engineering Ahead of Print / Just Accepted | SINTA - Science and Technology Index

Requires Authentication May 18, 2021
Advances in seawater membrane distillation (SWMD) towards stand-alone zero liquid discharge (ZLD) desalination
Helen Julian, Novesa Nurgirisia, Putu Doddy Sutrisna, I. Gede Wenten
Article number: 000010151520200073
More Cite this

Open Access April 27, 2021
Carbomer microgels as model yield-stress fluids
Zdzisław Jaworski, Tadeusz Spychaj, Anna Story, Grzegorz Story
Article number: 000010151520200016
More Cite this Download PDF

Requires Authentication April 21, 2021
Polyoxadiazoles as proton exchange membranes for fuel cell application
Yaroslav Kobzar, Kateryna Fatyeyeva, Corinne Chappey, Nicolas Désilles, Stéphane Marais
Article number: 000010151520200040
More Cite this

Requires Authentication April 20, 2021
Ignition–extinction analysis of catalytic reactor models
Vemuri Balakotaiah, Zhe Sun, Ram Ratnakar
Article number: 000010151520200113
More Cite this

2. Informasi tentang jurnal dan editorial board dari jurnal

degruyter.com

Edit item: Article #41280 - Ubaya Repository | in Chemical Engineering - v2.sherpa | Advances in seawater membrane distillation (S... | Engineering Ahead of Print / Just Accepted | SINTA - Science and Technology Index

DE G | Search De Gruyter | € EUR | EN | 0 | Log in

SUBJECTS SERVICES PUBLICATIONS ABOUT

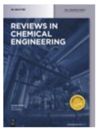

Published by De Gruyter

Ahead of Print / Just Accepted

Issue of Reviews in Chemical Engineering

Search journal

Ahead of Print / Just Accepted   All content

CONTENTS   **JOURNAL OVERVIEW**

About this journal

Objective

Reviews in Chemical Engineering publishes authoritative review articles on all aspects of the broad field of chemical engineering and applied chemistry. Its aim is to develop new insights and understanding and to promote interest and research activity in chemical engineering, as well as the application of new developments in these areas. The bimonthly journal publishes peer-reviewed articles by leading chemical engineers, applied scientists and mathematicians. The broad interest today in solutions through chemistry to some of the world's most challenging problems ensures that *Reviews in Chemical Engineering* will play a significant role in the growth of the field as a whole.

Topics

Cutting-edge topics such as but not limited to the following:

degruyter.com

Edit item: Article #41280 - Ubaya Repository | Reviews in Chemical Engineering - v2.sherpa | Advances in seawater membrane distillation (S... | Reviews in Chemical Engineering | SINTA - Science and Technology Index

DE G | Search De Gruyter | € EUR | EN | 0 | Log in

SUBJECTS SERVICES PUBLICATIONS ABOUT

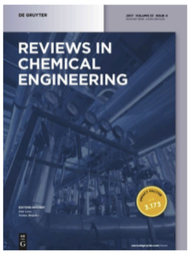

Published since January 1, 1982

Reviews in Chemical Engineering

ISSN: 2191-0235

Editors-in-chief: Dan Luss, Neima Brauner

Editorial Board: David Agar, Mark E. Davis, Thomas F. Edgar, Lidietta Giorno, J. B. Joshi, Johannes Khinast, Joseph Kost, L. Gary Leal, Jinghai Li, Patrick L. Mills, Massimo Morbidelli, Ka Ming Ng, Avi Schroeder, John Seinfeld, E. Hugh Stitt, Enrico Tronconi, Constantinos G. Vayenas, Peter Vekilov, Andrey Zagoruiko, Edwin Zondervan

Impact Factor: 6.299

OVERVIEW   LATEST ISSUE   ISSUES   RANKING   SUBMIT   **EDITORIAL**

Editorial

Editors-in-Chief

Dan Luss (Houston, TX, USA)

Neima Brauner (Tel Aviv, Israel)

Editorial Board

If you have institutional access, your institution may have a subscription to this journal. **Authenticate with your institution** to access content.

— or —

Subscription

Print Individual	713,00 €
Electronic Individual	99,00 €
Print + Electronic Individual	856,00 €
Print Institution	713,00 €
Electronic Institution	713,00 €
Print + Electronic Institution	856,00 €

To subscribe

Contact our sales team

degruyter.com

Edit item: Article #41280 - Ubaya Repository | Reviews in Chemical Engineering - v2.sherpa | Advances in seawater membrane distillation (S... | Reviews in Chemical Engineering | SINTA - Science and Technology Index

Editorial

Institution

To subscribe

Contact our sales team

Online ISSN: 2191-0235
Print ISSN: 0167-8299
Type: Journal
Language: English
Publisher: De Gruyter
First published: January 1, 1982
Publication Frequency: 8 Issues per Year
Audience: Chemical engineers; biochemical engineers; environmental engineers; researchers in applied chemistry; mathematicians

Search journal

degruyter.com

Edit item: Article #41280 - Ubaya Repository | Reviews in Chemical Engineering - v2.sherpa | Advances in seawater membrane distillation (S... | Reviews in Chemical Engineering | SINTA - Science and Technology Index

Joseph Kost (Beer Sheva, Israel)
Jinghai Li (Beijing, China)
L. Gary Leal (Santa Barbara, CA, USA)
Patrick L. Mills (Kingsville, TX, USA)
Massimo Morbidelli (Zurich, Switzerland)
Ka Ming Ng (Hong Kong, China)
Avi Schroeder (Haifa, Israel)
John H. Seinfeld (Pasadena, CA, USA)
E. Hugh Stitt (Cleveland, UK)
Enrico Tronconi (Milan, Italy)
Constantinos G. Vayenas (Patras, Greece)
Peter Vekilov (Houston, TX, USA)
Andrey N. Zagoruiko (Novosibirsk, Russia)
Edwin Zondervan (Bremen, Germany)

Editorial Office
Gunda Stöber
De Gruyter
Genthiner Str. 13
10785 Berlin, Germany
Tel. +49-30-26005-279
E-mail: rev.chem.eng.editorial@degruyter.com

Audience: Chemical engineers; biochemical engineers; environmental engineers; researchers in applied chemistry; mathematicians

Search journal

(Deutsch)

1. Bukti Journal Scopus Q1 dalam halaman website Scimagojr.com

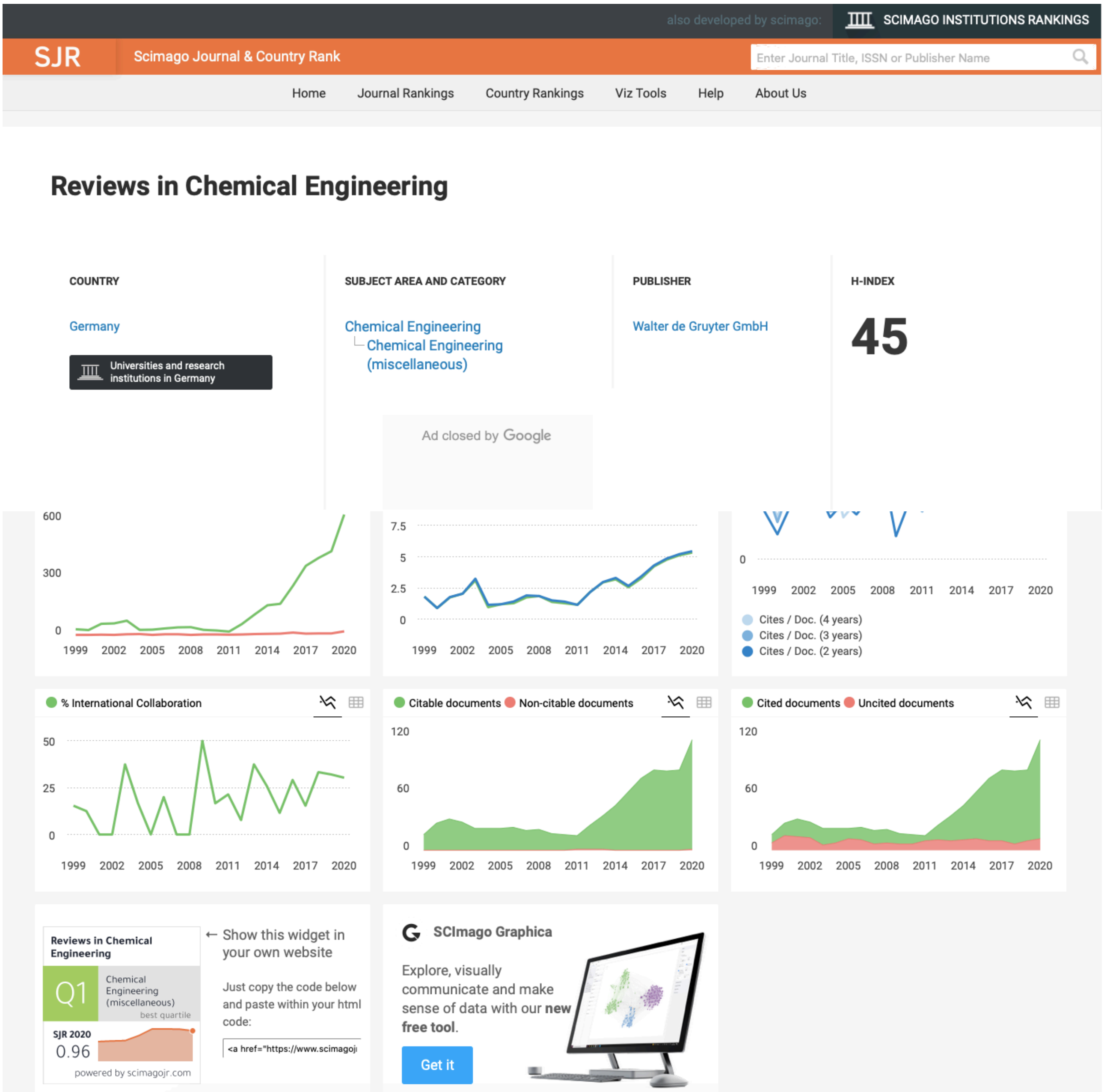

2. Bukti artikel dalam halaman Scopus penulis:

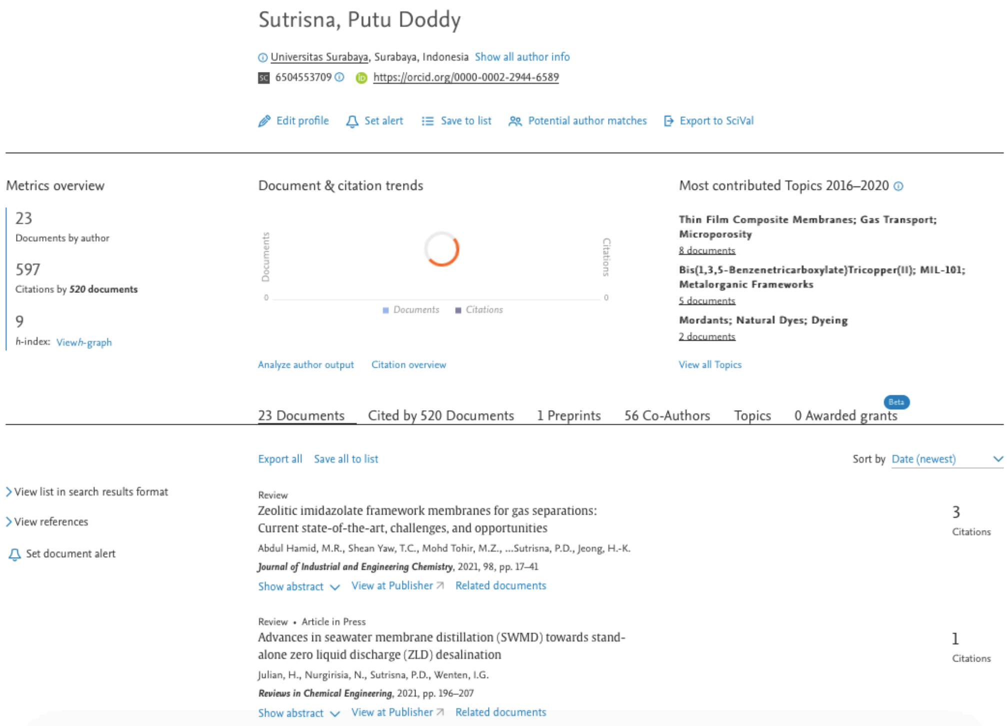
Sutrisna, Putu Doddy

Universitas Surabaya, Surabaya, Indonesia Show all author info

6504553709 https://orcid.org/0000-0002-2944-6589

Edit profile Set alert Save to list Potential author matches Export to SciVal

Metrics overview

23
Documents by author

597
Citations by 520 documents

9
h-index: View h-graph

Document & citation trends

Documents Citations

Analyze author output Citation overview

Most contributed Topics 2016–2020

Thin Film Composite Membranes; Gas Transport; Microporosity
8 documents

Bis(1,3,5-Benzenetricarboxylate)Tricopper(II); MIL-101; Metalorganic Frameworks
5 documents

Mordants; Natural Dyes; Dyeing
2 documents

View all Topics

23 Documents | Cited by 520 Documents | 1 Preprints | 56 Co-Authors | Topics | 0 Awarded grants

Export all Save all to list

Sort by Date (newest)

View list in search results format

View references

Set document alert

Review
Zeolitic imidazolate framework membranes for gas separations: Current state-of-the-art, challenges, and opportunities
Abdul Hamid, M.R., Shean Yaw, T.C., Mohd Tohir, M.Z., ...Sutrisna, P.D., Jeong, H.-K.
Journal of Industrial and Engineering Chemistry, 2021, 98, pp. 17–41
Show abstract View at Publisher Related documents
3 Citations

Review • Article in Press
Advances in seawater membrane distillation (SWMD) towards stand-alone zero liquid discharge (ZLD) desalination
Julian, H., Nurgirisia, N., Sutrisna, P.D., Wenten, I.G.
Reviews in Chemical Engineering, 2021, pp. 196–207
Show abstract View at Publisher Related documents
1 Citations

3. Bukti artikel dalam halaman Sinta penulis:

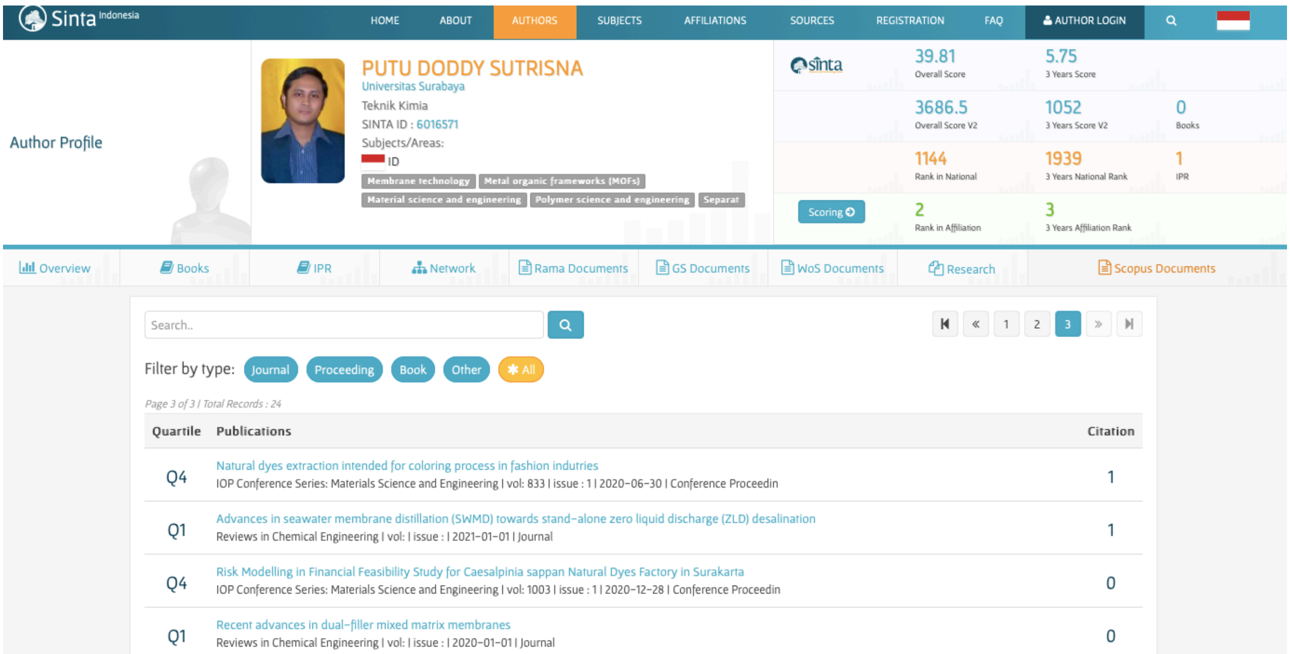
Sinta Indonesia | HOME | ABOUT | AUTHORS | SUBJECTS | AFFILIATIONS | SOURCES | REGISTRATION | FAQ | AUTHOR LOGIN

Author Profile

PUTU DODDY SUTRISNA
Universitas Surabaya
Teknik Kimia
SINTA ID : 6016571
Subjects/Areas:
ID
Membrane technology | Metal organic frameworks (MOFs) | Material science and engineering | Polymer science and engineering | Separat

sinta
39.81 Overall Score | 5.75 3 Years Score
3686.5 Overall Score V2 | 1052 3 Years Score V2 | 0 Books
1144 Rank in National | 1939 3 Years National Rank | 1 IPR
Scoring | 2 Rank in Affiliation | 3 3 Years Affiliation Rank

Overview | Books | IPR | Network | Rama Documents | GS Documents | WoS Documents | Research | Scopus Documents

Search..

1 2 3

Filter by type: Journal Proceeding Book Other All

Page 3 of 3 | Total Records : 24

Quartile	Publications	Citation
Q4	Natural dyes extraction intended for coloring process in fashion indutries IOP Conference Series: Materials Science and Engineering | vol: 833 | issue : 1 | 2020-06-30 | Conference Proceedin	1
Q1	Advances in seawater membrane distillation (SWMD) towards stand-alone zero liquid discharge (ZLD) desalination Reviews in Chemical Engineering | vol: | issue : | 2021-01-01 | Journal	1
Q4	Risk Modelling in Financial Feasibility Study for Caesalpinia sappan Natural Dyes Factory in Surakarta IOP Conference Series: Materials Science and Engineering | vol: 1003 | issue : 1 | 2020-12-28 | Conference Proceedin	0
Q1	Recent advances in dual-filler mixed matrix membranes Reviews in Chemical Engineering | vol: | issue : | 2020-01-01 | Journal	0

4. Copy halaman website yang memuat paper

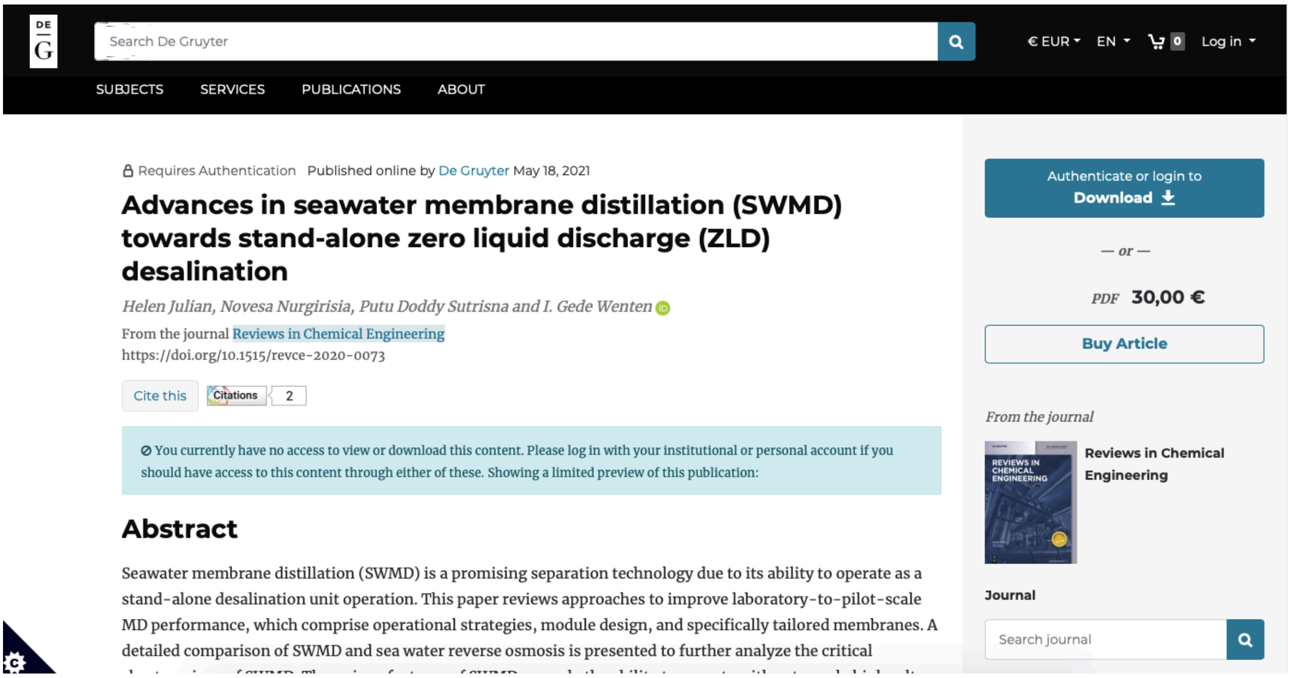

DE G

Search De Gruyter

€ EUR EN 0 Log in

SUBJECTS SERVICES PUBLICATIONS ABOUT

Requires Authentication Published online by De Gruyter May 18, 2021

Advances in seawater membrane distillation (SWMD) towards stand-alone zero liquid discharge (ZLD) desalination

Helen Julian, Novesa Nurgirisia, Putu Doddy Sutrisna and I. Gede Wenten

From the journal Reviews in Chemical Engineering

https://doi.org/10.1515/revce-2020-0073

Cite this Citations 2

You currently have no access to view or download this content. Please log in with your institutional or personal account if you should have access to this content through either of these. Showing a limited preview of this publication:

Abstract

Seawater membrane distillation (SWMD) is a promising separation technology due to its ability to operate as a stand-alone desalination unit operation. This paper reviews approaches to improve laboratory-to-pilot-scale MD performance, which comprise operational strategies, module design, and specifically tailored membranes. A detailed comparison of SWMD and sea water reverse osmosis is presented to further analyze the critical

Authenticate or login to Download

— or —

PDF 30,00 €

Buy Article

From the journal

Reviews in Chemical Engineering

Journal

Search journal